AD-A042 443 PRATT AND WHITNEY AIRCRAFT GROUP WEST PALM BEACH FLA --ETC F/G 11/6
WEAR RESISTANT COATINGS FOR TITANIUM ALLOYS.(U)
MAR 77 B A MANTY, H R LISS N00019-76-C-0342
UNCLASSIFIED FR-8400 NL

| OF |
AD
A042443

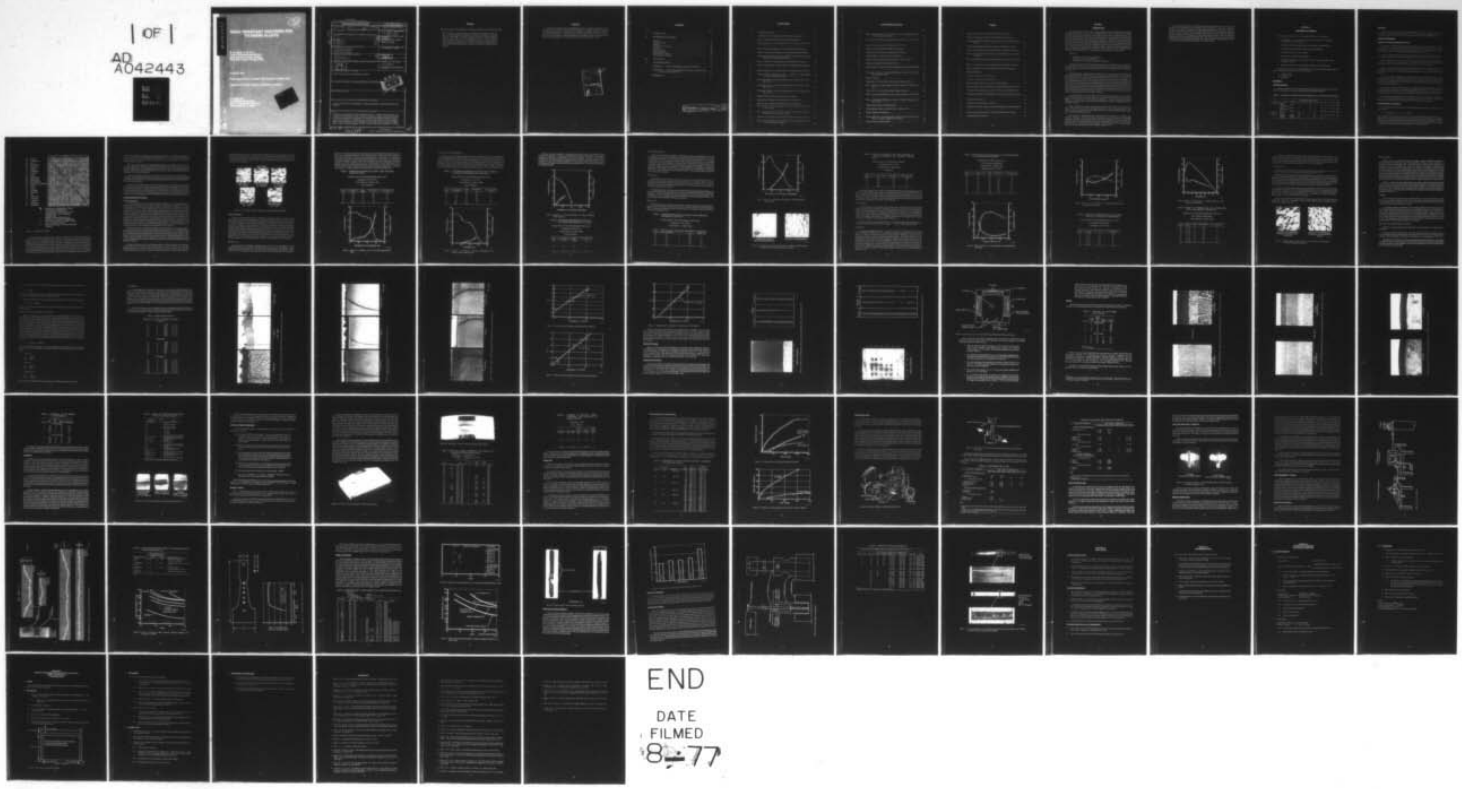

END

DATE
FILMED
8-77

12

B.S.

WEAR RESISTANT COATINGS FOR TITANIUM ALLOYS

B. A. Manty, H. R. Lisa
Pratt & Whitney Aircraft Group
Government Products Division
West Palm Beach, Florida 33402

15 March 1977

Final Report Period 15 March 1976 through 15 March 1977

Approved for public release; distribution unlimited

Prepared for
Department of the Navy
Naval Air Systems Command
Washington, D. C. 20361

UNCLASSIFIED

SECURITY CLASSIFICATION OF THIS PAGE *(When Data Entered)*

REPORT DOCUMENTATION PAGE

READ INSTRUCTIONS BEFORE COMPLETING FORM

1. REPORT NUMBER: N00019-76-C-0342 (9) Final Rept. 15 Mar 76-15 Mar 77	2. GOVT ACCESSION NO.
3. RECIPIENT'S CATALOG NUMBER	
4. TITLE (and Subtitle): (6) WEAR RESISTANT COATINGS FOR TITANIUM ALLOYS	5. TYPE OF REPORT & PERIOD COVERED: Final March 15, 1976 - March 15, 1977
6. PERFORMING ORG. REPORT NUMBER: (14) FR-8400	
7. AUTHOR(s): (10) B. A. Manty, H. R. Liss	8. CONTRACT OR GRANT NUMBER(s): (15) N00019-76-C-0342
9. PERFORMING ORGANIZATION NAME AND ADDRESS: United Technologies Corporation, Pratt & Whitney Aircraft Group, Government Products Division, West Palm Beach, Florida 33402	10. PROGRAM ELEMENT, PROJECT, TASK AREA & WORK UNIT NUMBERS
11. CONTROLLING OFFICE NAME AND ADDRESS: Department of Navy, Naval Air Systems Command, Washington, D. C. 20361	12. REPORT DATE: (14) March 1977
	13. NUMBER OF PAGES: 73
14. MONITORING AGENCY NAME & ADDRESS *(if different from Controlling Office)*: (12) 74p.	15. SECURITY CLASS. *(of this report)*: UNCLASSIFIED
	15a. DECLASSIFICATION/DOWNGRADING SCHEDULE

16. DISTRIBUTION STATEMENT *(of this Report)*

Approved for public release; distribution unlimited.

17. DISTRIBUTION STATEMENT *(of the abstract entered in Block 20, if different from Report)*

18. SUPPLEMENTARY NOTES

19. KEY WORDS *(Continue on reverse side if necessary and identify by block number)*

Coating, Titanium Alloys, Wear Resistant, Chromium-Molybdenum, Electroplating, Sputtering, Diffusion

20. ABSTRACT *(Continue on reverse side if necessary and identify by block number)*

Techniques for applying chromium-molybdenum alloys to titanium alloy substrates were developed and the resultant systems evaluated as protective coatings. Deposition techniques including electroplating and sputtering were considered and diffusion properties studied. A coating alloy containing 1% molybdenum was shown to greatly improve the wear resistance. Erosion, oxidation and stress corrosion properties were also improved. The coating system had no apparent effect on fatigue properties of Ti 8Al-1V-1Mo at either room temperature or 315°C.

DD FORM 1 JAN 73 1473 EDITION OF 1 NOV 65 IS OBSOLETE

392887

UNCLASSIFIED

SECURITY CLASSIFICATION OF THIS PAGE *(When Data Entered)*

PREFACE

The authors wish to acknowledge the contribution provided by the following individuals:

Mr. H. Lada for his diligence in conducting the plating studies and Mr. R. J. Hecht and Mr. R. J. Mullaly for the sputter application of coatings. Mr. W. Tress and Mr. W. Morgan conducted analysis of the deposits/plating solutions and aided in the interpretation of the results obtained. Mr. S. Bonifazi contributed with suggestions leading to the development of coating application techniques. Mr. J. Hoffner, NAVAIR, provided technical monitoring of the program and advice helpful to the successful completion of this program.

ABSTRACT

Techniques for applying chromium-molybdenum alloys to titanium alloy substrates were developed and the resultant systems evaluated as protective coatings. Deposition techniques including electroplating and sputtering were considered and diffusion properties studied. A coating alloy containing 1% molybdenum was shown to greatly improve the wear resistance. Erosion, oxidation and stress corrosion properties were also improved. The coating system had no effect on fatigue properties of Ti 8Al-1V-1Mo at either room temperature or 315°C.

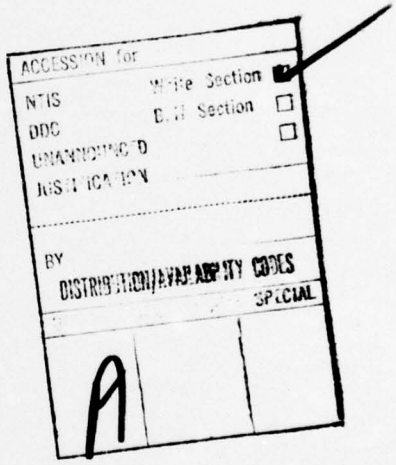

CONTENTS

ILLUSTRATIONS

ILLUSTRATIONS (Continued)

TABLES

SECTION I

INTRODUCTION

The effective use of titanium alloys in advanced engine and airframe applications is strongly dependent upon surface treatment and coatings. This has been a continuing chemical and metallurgical concern since titanium was first applied to gas turbine engine service in the early 1950's. As engine experience and laboratory testing progressed, specific problems were identified, namely erosion, fretting, galling and corrosion. These were alleviated by surface treatments designed to deal with the specific engineering environments. Coatings are still tailored to meet problems, and alloy compositions and treatments are adjusted to optimize mechanical properties and minimize corrosion susceptibility. Meanwhile, alloy developments during the last decade have continued to raise the allowable temperature limits of titanium alloys. Further progress is expected, extending development goals to a 650°C (1200°F) capability. Three principal obstacles hinder the maximum application of titanium alloys in advanced gas turbine engines.

These are:

1. Resistance to wear, fretting and galling
2. Hot-salt stress corrosion resistance
3. Resistance to air oxidation at elevated temperatures.

The program described in the following sections was directed toward solution of these three key problems. If coating systems are not developed to protect against these environments, designers will be denied the weight advantages which emerging high-temperature titanium alloys could provide.

Coatings previously investigated for the protection of titanium from wear, fretting and galling have included electrodeposits of silver, nickel and chromium (Reference 1). These studies demonstrated that some degree of protection could be achieved with any of the coatings, but other problems such as silver induced corrosion (or stress corrosion) and the coatings effect on basic engineering properties were not completely dealt with. Other investigators (Reference 2) have shown a six-fold improvement in wear life achieved by using a chromium-molybdenum alloy electrodeposit on steel rather than a more conventional chromium plate. These alloys had, however, never been tailored for use on titanium alloys. Other wear resistance coatings such as anodize (Reference 3) has shown promise but only when used with dry film lubrication. This, and other less successful anodic and conversion coatings, do not provide the overall resistance to wear, fretting and galling achievable with metallic coatings.

Coatings deposited on titanium alloys that have exhibited resistance to erosion include nickel, chromium, aluminum, silicon, (Reference 4), chemical vapor deposited titanium carbide (Reference 5) and a titanium carbonitride coating applied over electroless nickel plated titanium (Reference 6). Unfortunately, most of these erosion resistant coatings also significantly reduced the fatigue strength.

Nickel, aluminum and anodic coatings have all shown some ability to protect titanium alloys from hot-salt stress corrosion cracking (References 7 and 3). Diffused aluminum, zinc, chromium, silicon, and plasma sprayed aluminum have also protected titanium alloys under some conditions (References 8 and 9).

Several types of coatings have been investigated for the protection of titanium from oxidation. These have included aluminides, silicides and various other types of intermetallic compounds normally used to protect nickel alloy turbine hardware. In every case, although oxidation protection was demonstrated, many times to temperatures above 650°C (1200°F), other problems such as reduced mechanical properties or enhanced sensitivity to environmentally enhanced cracking, precluded their use on hardware (Reference 10).

In this program, techniques for applying a chromium-molybdenum alloy to titanium alloy substrates were developed and the resultant systems evaluated as protective coatings for titanium alloys. Deposition techniques including electroplating and sputtering were considered and diffusion properties studied. Previous work indicated that the coatings could be applied to titanium alloys to provide a wear resistant surface without severely affecting mechanical properties. Therefore, these coatings were selected for further evaluation. This work completes the first phase of an anticipated three-phase effort. The second will strive for a more complete characterization of the coating and application to a sample part while the final phase will scale-up the process and provide production parts for in-service testing.

SECTION II

EXPERIMENTAL PROGRAM

The experimental portion of this program was divided into several sections:

1. Development of a procedure to deposit two compositions of chromium-molybdenum onto titanium alloys
2. Evaluate the diffusion characteristics of the coating into titanium alloys
3. Evaluate alternate applications methods such as sputtering
4. Evaluate the adhesion of the coatings
5. Evaluate the erosion and wear resistance
6. Determine the effects of the coating on stress corrosion resistance and oxidation properties
7. Measure the fatigue and fretting-fatigue properties of the coated alloys.

The object of this first phase of development was to provide a recommended procedure to apply a chromium-molybdenum coating to three alloys:

1. Ti 8Al-1V-1Mo
2. Ti 6Al-6V-2Sn
3. Ti 6Al-4V

MATERIALS

Substrate Materials

Chemical compositions of the substrate materials used in this investigation are listed in Table 1. The compositions were all confirmed by Pratt & Whitney Aircraft.

TABLE 1. CHEMICAL COMPOSITION OF TITANIUM ALLOY SUBSTRATE MATERIALS

			Composition, Percent by Weight										
Alloy	*Test*	*Heat Code*	*Al*	*Sn*	*Zr*	*Mo*	*V*	*Cr*	*Fe*	*N*	*C*	*O*	*H*
Ti 8Al-1V-1Mo	Plating Diffusion Stress Corrosion	MNEJ	7.9	-	-	1.1	1.0	-	0.06	0.010	0.02	0.10	0.0085
	Fatigue Fretting-Fatigue	BCVJ	7.5	-	-	1.0	1.0	-	0.10	0.011	0.023	0.16	0.006
	Erosion	BCVK	8.2	-	-	1.1	1.1		0.08	0.009	0.02	0.106	0.0057
Ti 6Al-6V-2Sn	Diffusion	-	5.6	2.5	-	-	5.8	-	-	-	-	-	-
Ti 6Al-4V	Diffusion	BZXY	5.8	-	-	-	4.0	-	0.12	0.010	0.024	0.13	0.011
	Adhesion	N-3618	6.2	-	-	-	3.7	-	0.15	-	-	-	-
	Oxidation	N-3623	6.2	-	-	-	3.6	-	0.11	-	-	-	-

Chemicals

Chemicals used in preparing the plating solutions and other solutions used in this investigation were all reagent grade materials except for the self-regulating chromic acid which was obtained from United Chromium Corporation under their designation SRHS CR 110.

COATING PROCESSES

Selection of Chromium-Molybdenum Alloys

The first interest P&WA had in chromium-molybdenum coatings stemmed from a cryogenic wear problem on a rocket engine flow divider valve (AISI 347). Conventional, hard chromium electroplate was not providing the required wear resistance; therefore, a number of other coatings were evaluated, of which the chromium-molybdenum proved to be the best.

Literature references dating back more than 20 years on the codeposition of chromium and molybdenum exist although no industrial applications other than this instance were found.

Dense, adherent deposits with high corrosion and wear resistance can be obtained by this codeposition. The success of these deposits, as reported in the literature, can probably be attributed to the unique combination of properties not possessed by any material.

One of the more significant results that have been obtained is the effect of about 1% molybdenum in chromium increasing the wear resistance by 3 to 8 times (Reference 13). Molybdenum appears not only to improve the wear resistance but also to improve the corrosion resistance.

Literature references describing the deposition of alloys containing as much as 22% molybdenum have been found (Reference 14) but errors in analytical procedures uncovered in subsequent work indicate deposits have generally not contained more than 2% molybdenum. All investigations have reported the current efficiency decreased as the molybdenum content of the deposit increased (Reference 15).

The selection of chromium-molybdenum as a coating system for titanium alloys was based on the apparent chemical and metallurgical compatibility perhaps best illustrated by the weldability chart shown as Figure 1. This compatibility feature was believed a crucial factor in minimizing effects of the coating process on mechanical properties such as fatigue strength.

Further, excellent elevated temperature oxidation resistance of chromium -5% molybdenum alloys has been reported (Reference 16) to temperatures above 927°C (1700°F), a temperature greater than the highest expected temperature for the coating on titanium alloys.

Electrodeposition of Chromium

The overall reaction resulting in chromium deposition from aqueous solution can be represented by:

$$[Cr^{+6}(H_2O)n]_{sol} + 6e^{-} \rightarrow Cr_{lattice} + nH_2O$$

This simplified form represents the reduction of a hydrated hexavalent chromium ion to a chromium atom in the crystal lattice. Previous studies with tracers by Brenner and Ogburn (Reference 11) confirmed that chromium was deposited directly from the hexavalent state. Even so, several steps must be involved in the overall reaction and no comprehensive theory is available to explain why chromium deposits are obtained from a chromic acid bath.

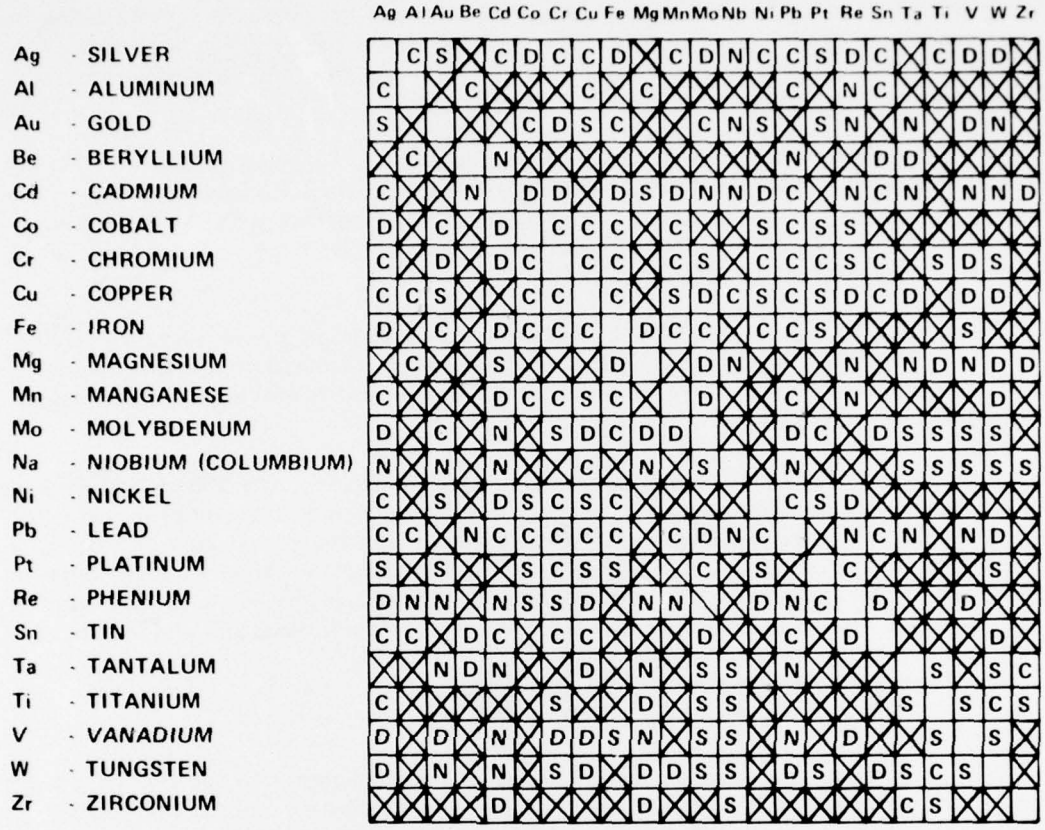

Figure 1. Compatibility of Metal

Chromium cannot be deposited from a solution containing only chromic acid and water without one or more acid radicals acting as catalysts to bring about the deposition. Without the catalysis, it has been suggested (Reference 12) that an insoluble film of chromium chromate, $Cr(OH)CrO_4$ forms on the cathode. A film of this type is considered to prevent the deposition of chromium, and the addition of a catalyst is believed to modify the film allowing electrodeposition. Typically, sulfates and more recently fluorides (frequently in the form of a complex fluoride such as SiF_6 hexafluorosilicate) are used as catalysts. The ratio of chromic acid to catalysts is generally maintained at about 100:1. Self-regulating chromium plating solutions were introduced to eliminate the need for maintaining the correct catalyst concentration by periodic analysis.

Usually, they depend on the addition of a sparingly soluble sulfate to the bath which supplies the correct amount of SO_4^{-2} automatically. Self-regulating baths are generally used throughout industry so they were used in this work except where other catalyst and catalyst concentration effects were being studied.

While the current efficiency in chromium plating baths is low, usually 10 to 20%, a fairly high rate of deposition is obtained owing to the relatively high current densities used. Voltages are generally higher than other electroplating processes which, together with the higher current densities, would seem a disadvantage. These factors have not, however, seriously hindered the widespread use of chromium plating.

Chromium plating baths have a relatively poor throwing power (covering ability). Regardless, remarkably good results have been achieved even in the plating of irregular shapes when the process is carefully controlled and auxiliary anodes and thieves are used in accordance with well-known principles.

Insoluble lead-tin anodes were used in all our plating studies. The film of lead peroxide which forms on these anodes during use causes any trivalent chromium formed on the cathode to be reoxidized continuously to chromic acid, thereby maintaining its concentration at a low value. Pure lead can be used as an anode material but it will be attacked by the solution and cause the formation of excessive amounts of a lead chromate sludge. Lead-tin alloys have the best corrosion resistance so are recommended as the best available material for both anodes and heating coils.

Coating Deposition Parameters

Surface Preparation

Several preparations were considered as surface pretreatments to the plating process. Ideally, this surface should be clean, free of interface contamination and activated so that an electrodeposit will adhere without further treatment. Unfortunately, titanium is not easily activated because of its rapidly forming oxides. Previous in-house studies and test results reported later on Table 13 have demonstrated that suitable adhesion cannot be obtained without a diffusion treatment after plating. The most sophisticated treatments, such as conversion of the surface to hydrides, or complexing the surface with tartrates to minimize oxide formation, have not resulted in bond strengths above 55.2 MN/m² (8 ksi). Treatments such as abrading while plating or inert atmosphere plating do not significantly improve the results. For these reasons, the intent of our surface preparation studies was to find a method producing a contaminant-free surface which would not passivate during plating. The adhesion of as-plated deposit had to be sufficient to hold the plate on during normal handling and until a subsequent diffusion cycle could be performed to metallurgically bond the coating to the substrate.

Generally, plating over a vapor blasted surface worked satisfactorily, but the surface had to be kept wet between vapor blasting and plating and occasionally, for no apparent reason, localized passivation prevented deposition. Grit blasting with from 80 to 240 grit silicon carbide prior to plating resulted in excellent adhesion of the chromium-molybdenum electrodeposits. The problem with this pretreatment was that abrasive particles imbedded themselves into the titanium surface resulting in excessive interface contamination. These abrasive particles would not only interfere with any subsequent diffusion treatment, but also reduce the life of the coating during wear testing.

Ultimately, the best solution to providing consistently satisfactory surfaces involved vapor blasting with Novaculite 200 (aluminum oxide) abrasive at 0.35-0.7 MN/m² (50 to 100 psig) pressure followed by a chromium conversion coating. The conversion coating was applied by immersing the titanium parts into a solution containing hydrofluoric acid and sodium chromate.

Scanning electron microscope examination of the surfaces after each step in the process and the results of hydrogen analysis are shown in Figure 2. Microprobe analysis confirmed the presence of chromium on the surfaces after treatment in the acid chromate solution. The hydrogen analysis results confirmed that less than 100 ppm increase in hydrogen content was caused by this combination of treatments.

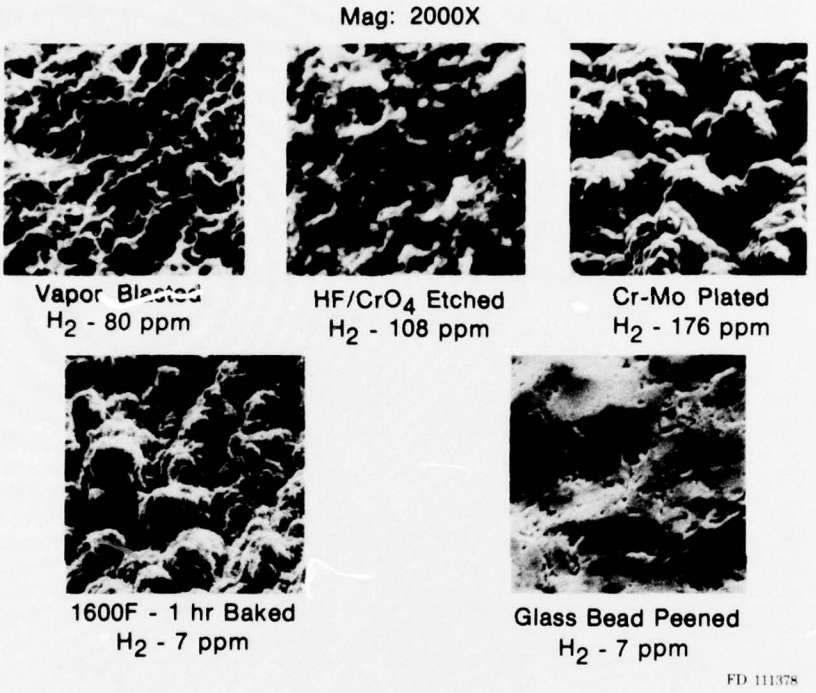

Figure 2. Ti 8Al-1Mo-1V Surface Appearance After Each Processing Step

Plating Conditions

This part of the investigation was conducted to establish conditions required for both maintaining a reasonable cathode efficiency and providing controlled quantities of molybdenum in the deposits. Most of the work was done in standard, self-regulating, chromium plating baths into which molybdenum was added as molybdic acid, anodically dissolved molybdenum, ammonium molybdate, or sodium molybdate. Typical baths consisted of 300 g/l self-regulating chromic acid containing various amounts of the molybdenum in solution. Trivalent chromium contents did not exceed 2 g/l and were maintained at these low values by using large anode to cathode ratios. Samples were prepared and plated at the specified temperature, current density and conditions for that test. During plating, the temperatures were maintained within $\pm 2°C$. After plating, the samples were rinsed and dried. Weights before and after plating were used together with total ampere-minutes during plating to calculate the cathode efficiency. Microprobe analysis was used for quantitative analysis of the molybdenum in the deposits.

Molybdic Acid

Varying amounts of molybdic acid ranging from 20 to 122.7 g/l were added to a self-regulating chromium plating bath containing 300 g/l chromic acid. Molybdenum started codepositing with the chromium with only 20 g/l added. The amount in the deposit increased slowly up to 0.6% with about 80 g/l molybdic acid in solution. Raising the concentration in

solution to about 100 g/l increased the molybdenum in the electrodeposit to greater than 2% but there was a corresponding reduction in the cathode efficiency. Table 2 provides a summary of these results and Figure 3 depicts the results graphically. In that figure, the molybdenum concentration in solution is expressed in g/l molybdenum rather than molybdic acid. This method compares the different methods of dissolving molybdenum since each figure has molybdenum expressed in the same units along the "x" axis. Substantial amounts of molybdenum could not be deposited with a reasonable cathode efficiency with molybdic acid and further study was not warranted. These results compared favorably with other investigations (Reference 17) conducted using molybdic acid (MoO_3) additions in a more dilute chromic acid plating bath.

TABLE 2. CHROMIUM-MOLYBDENUM PLATING USING MOLYBDIC ACID IN SOLUTION

Plating Solution: 300 g/l Self-regulating Chromic Acid

Temperature: 46°C (115°F)

Current Density: 47 ASD (3 ASI)

Time: 30 Minutes

Sample Number	*Solution Composition, g/l MoO_3*	*Plating Voltage, V*	*Cathode Efficiency, %*	*Composition of Deposit, % Mo*
133	20	5	21.3	0.2
134	40.9	5.6	18.6	0.3
135	61.4	5.4	17.6	0.3
136	81.8	5.4	17.2	0.6
137	102.3	5.6	2.0	2.1
138	122.7	5.6	0.4	-

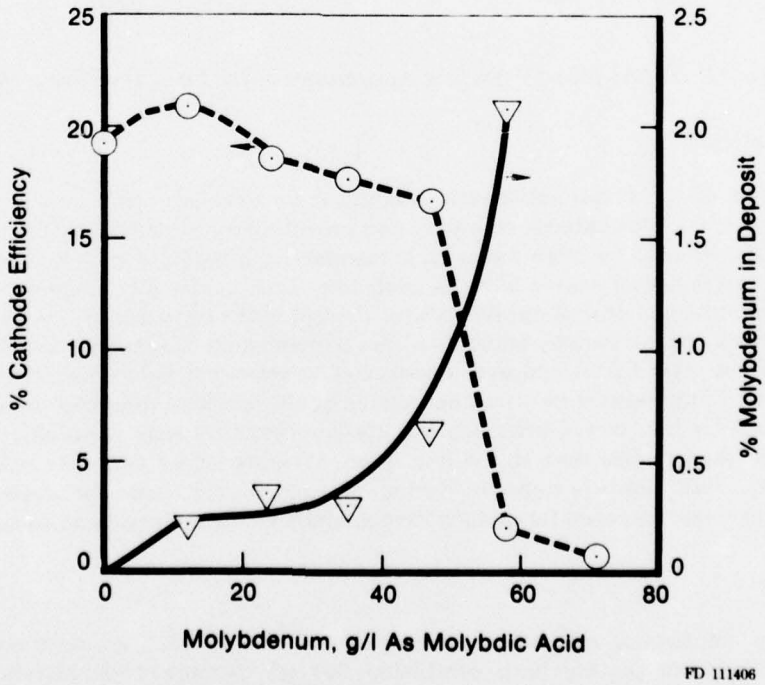

Figure 3. Influence of Molybdic Acid on Chromium-Molybdenum Plate

Anodically Dissolved Molybdenum

The earliest work discussing deposition of chromium-molybdenum alloys used anodically dissolved molybdenum as its additive (Reference 18). In our study, no molybdenum was observed in the electrodeposit until a little over 20 g/l molybdenum was dissolved in the chromic acid plating solution. As with the molybdic acid, the percent molybdenum increased as the molybdenum content of the solution increased, but cathode efficiencies decreased. Table 3 and Figure 4 summarize these results. Deposits formed from plating baths containing anodically dissolved molybdenum did not show significant promise relative to other solutions evaluated.

TABLE 3. CHROMIUM-MOLYBDENUM PLATING USING ANODICALLY DISSOLVED MOLYBDENUM IN SOLUTION

Plating Solution: 300 g/l Self-regulating Chromic Acid

Temperature: 47°C (117°F)

Current Density: 47 ASD (3 ASI)

Time: 30 Minutes

Sample Number	*Solution Composition, g/l Molybdenum*	*Voltage, V*	*Cathode Efficiency, %*	*Composition of Deposit % Mo*
68	0	4.8	19.0	0
69	6.7	4.8	20.7	0
70	13.3	4.8	19.9	0
71	27.5	4.4	14.9	0
72	41.4	4.5	14.8	0.2
73	55.2	4.8	6.0	0.5
74	68.8	4.8	0	-

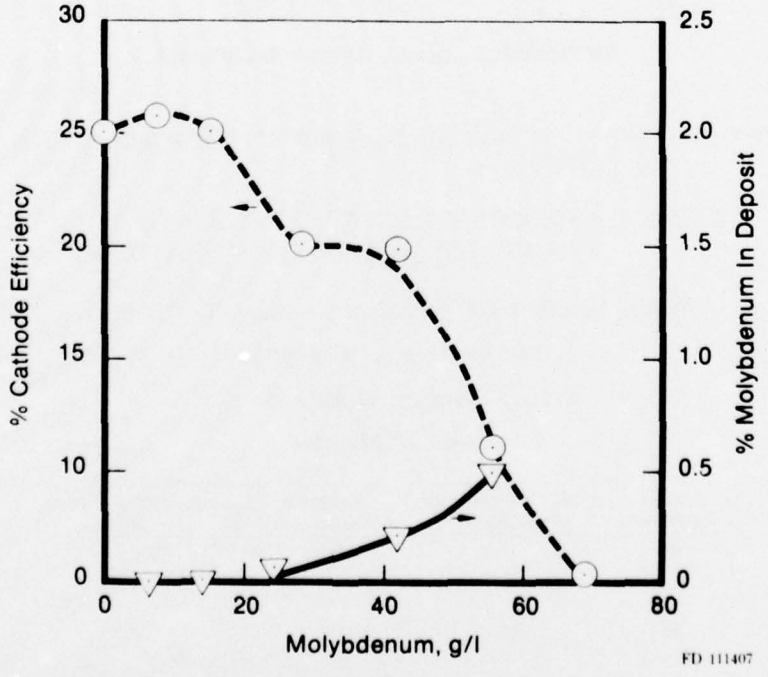

Figure 4. Influence of Anodically Dissolved Molybdenum on Chromium Molybdenum Plate

Addition of sodium molybdate to self-regulating, 300 g/l, chromic acid plating solutions, resulted in the deposition of chromium-molybdenum alloys (Figure 5 and Table 4). As expected, increasing concentrations of molybdenum in solution increased the amount in the deposit. Unfortunately, the cathode efficiency decreased faster with sodium molybdate additions than it did with any other way of putting molybdenum in the plating solution. By the time 40 g/l of molybdenum was added, the cathode efficiency had dropped to zero. This method was therefore not considered further.

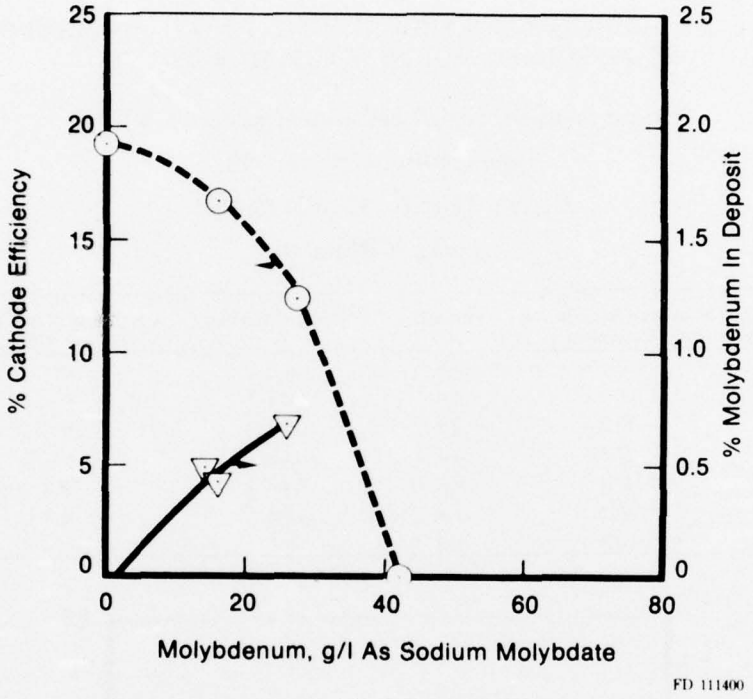

Figure 5. Influence of Sodium Molybdate on Chromium-Molybdenum Plating

TABLE 4. CHROMIUM-MOLYBDENUM PLATING USING SODIUM MOLYBDATE IN SOLUTION

Plating Solution: 300 g/l Self-regulating Chromic Acid

Temperature: 49°C (120°F)

Current Density: 47 ASD (3 ASI)

Time: 30 Minutes

Sample Number	*Solution Composition, g/l Na_2MoO_4*	*Cathode Efficiency, %*	*Composition of Deposit, % Mo*
65	34	16.9	0.4
66	68	11.6	0.7
67	102	0	-

Ammonium Molybdate

Above 25 g/l ammonium molybdate, corresponding to about 12 g/l molybdenum, in 300 g/l self-regulating chromic acid, molybdenum-containing deposits were obtained. At 75 g/l, 1% molybdenum deposits were consistently obtained with cathode efficiencies still 12 to 13%. Higher concentrations in solution reduced cathode efficiencies below practical levels, but did further increase the amount of molybdenum in deposits. Table 5 and Figure 6 summarize these results. It was learned that the best results were obtained with solutions containing 75 g/l ammonium molybdate. Larger amounts decreased the cathode efficiency and resulted in nonuniform appearances. Interestingly, at these concentrations the deposits obtained showed significantly fewer cracks than conventional chromium plate (Figure 7). This would explain the reported improved corrosion resistance.

Chromic Acid

The concentration of chromic acid used in conventional chromium plating ranges from 150 to 500 g/l. If the trivalent chromium content exceeds 10 g/l a gray nodular deposit is formed. Trivalent chromium alone cannot be used to deposit chromium from aqueous solutions. Our own evaluation of tetrachromate plating baths (Reference 19) for depositing chromoim-molybdenum alloys were completely unsuccessful.

Comparing the effects of chromic acid concentration from self-regulating salt additions, the range of 300 to 400 g/l seems acceptable from both the cathode efficiency and deposit composition as shown in Table 6. All these solutions were made with 75 g/l ammonium molybdate. The molybdenum content of the deposit increased by either increasing or decreasing the chromic acid concentration, but the cathode efficiency also decreased.

Sulfuric Acid

The electrodeposition of chromium from chromic acid takes place only in the presence of a catalyst. The most common of these, the sulfate ion, was used in this study. Our investigations with fluoride and complex fluoride catalysts showed them not as suitable as sulfate for depositing chromium-molybdenum alloys.

TABLE 5. CHROMIUM-MOLYBDENUM PLATING USING AMMONIUM MOLYBDATE IN SOLUTION

Plating Solution: 300 g/l Self-regulating Chromic Acid

Temperature: 49°C (120°F)

Current Density: 47 ASD (3 ASI)

Sample Number	*Solution Composition, g/l Ammonium Molybdate*	*Plating Voltage, V*	*Cathode Efficiency, %*	*Composition of Deposit, % Mo*
38	12.5	5	20.4	0
39	12.5	5	20.7	0
40	25.0	5	24.4	0
41	50.0	5	17.6	0.4
42	75.0	5	12.8	0.8
43	75.0	5	12.7	1.0
44	125.0	6	1.2	2.1

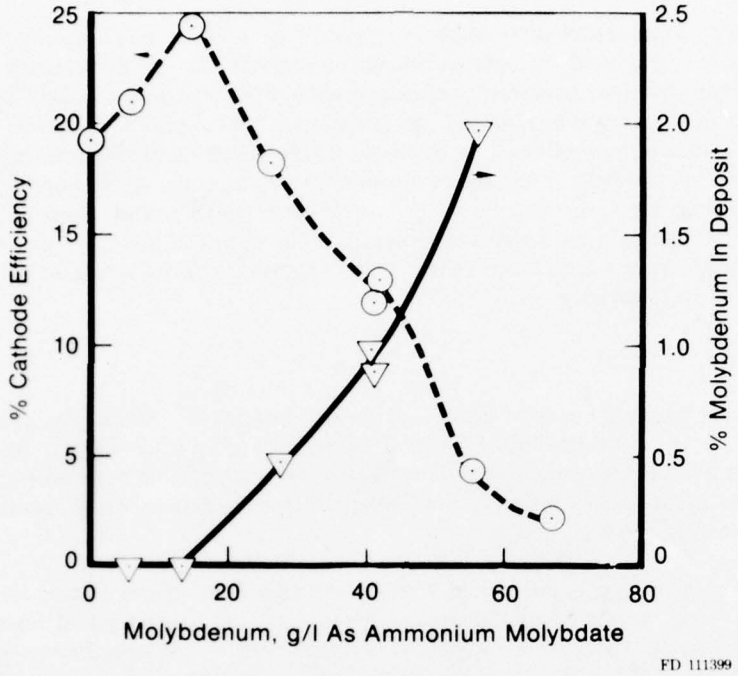

Figure 6. Influence of Ammonium Molybdate on Chromium-Molybdenum Plating

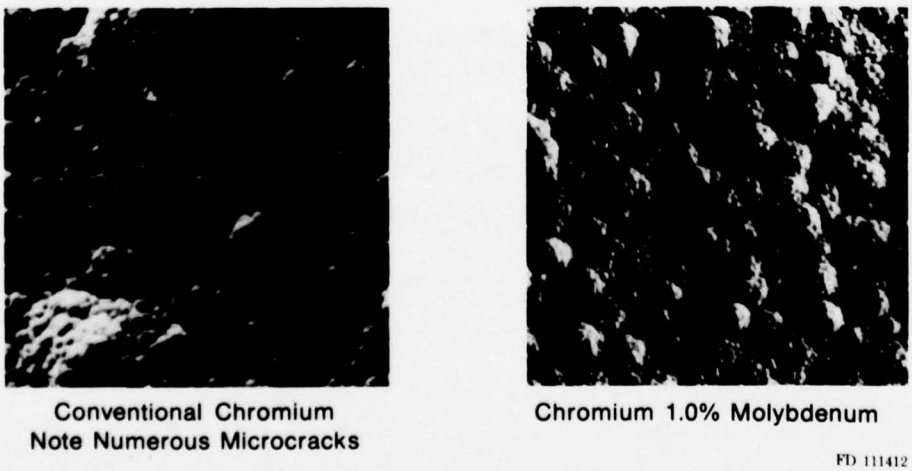

Figure 7. Scanning Electron Microscope Views at 1000X of As-Electroplated Chromium and Chromium-Molybdenum Deposits

TABLE 6. EFFECTS OF CHROMIC ACID CONCENTRATION ON CATHODE EFFICIENCY AND DEPOSIT COMPOSITION

Plating Solution: 75 g/l Ammonium Molybdate

Temperature: 49°C (120°F)

Current Density: 47 ASD (3 ASI)

Voltage: 5V

Sample Number	*Chromic Acid Concentration, g/l*	*Cathode Efficiency, %*	*Composition of Deposit, % Mo*
47	200	4.3	1.3
48	300	13.6	1.0
49	400	14.2	1.1
50	450	2.5	1.7
51	600	1.2	0

Controlled concentrations of sulfate ion were added stepwise to a solution made up with 300 g/l chromic acid (Reagent grade) and 75 g/l ammonium molybdate. The results are shown on Table 7 and Figure 8. Increasing sulfate concentration decreased the molybdenum content of the deposits. This was not unexpected since the cathode efficiency increased, and every time in the past when the cathode efficiency increased, the percent molybdenum decreased. For successful operation, the concentration of catalyst must be kept low.

Current Density

Using the solution that appeared most suitable and containing 300 g/l self-regulating chromic acid and 75 g/l ammonium molybdate, the effects of current density were determined. Figure 9 and Table 8 summarize the results. Reasonable cathode efficiencies with little difference in the amount of molybdenum in the deposit was observed over the range of 31 to 109 ASD (2 to 7 ASI). At 15.5 ASD (1 ASI), the cathode efficiency was lower, resulting in higher molybdenum content in the deposit and between 31 to 109 ASD, there seemed to be a slight trend to increase molybdenum in deposits as the current density increased.

Hull cell tests were also conducted on the 1% molydenum electroplate. Results indicate satisfactory plating can be obtained over the range of 11ASD (0.7ASI) to 62ASD (4ASI).

Temperature

Varying the temperature between −10 and 70°C was shown to influence both the cathode efficiency and the molybdenum content of the deposit. Maximum cathode efficiency occurred at about 0°C. Figure 10 and Table 9 summarize these results. Although a slight dip in the molybdenum content occurred at maximum cathode efficiency, the general trend was for the molybdenum content to decrease as the temperature increased. In fact, for the first time, as the cathode efficiency dropped, so did the molybdenum content. This occurred over the range of temperature from 10 to 50°C. This phenomenon is explained if we remember the plating bath contains self-regulating salts which no doubt increase in solubility as the temperature increases. This, in effect, increases the sulfate concentration which, in turn, decreases the molybdenum in the deposit as shown in Figure 8. The cathode efficiency dropped to zero as the temperature increased to 70°C.

TABLE 7. EFFECTS OF SULFATE CATALYSIS ON CATHODE EFFICIENCY AND DEPOSIT COMPOSITION

Plating Solution: 300 g/l Chromic Acid

75 g/l Ammonium Molybdate

Current Density: 47 ASD (3 ASI)

Temperature: 49°C (120°F)

Sample Number	*Sulfuric Acid Concentration, ml/l*	*Voltage, V*	*Cathode Efficiency, %*	*Composition of Deposit, % Mo*
84	0	4.6	0	-
126	0.5	5.0	1.8	1.3
127	0.75	5.0	14.2	0.6
128	1.0	5.0	14.7	0.5
129	1.25	4.8	16.1	0.3
130	1.5	4.8	15.8	0.3
131	1.75	4.8	17.1	0.2
132	2.0	4.8	19.2	0.1
91	3.6	4.6	14.5	0.3
93	6	4.4	3.1	0

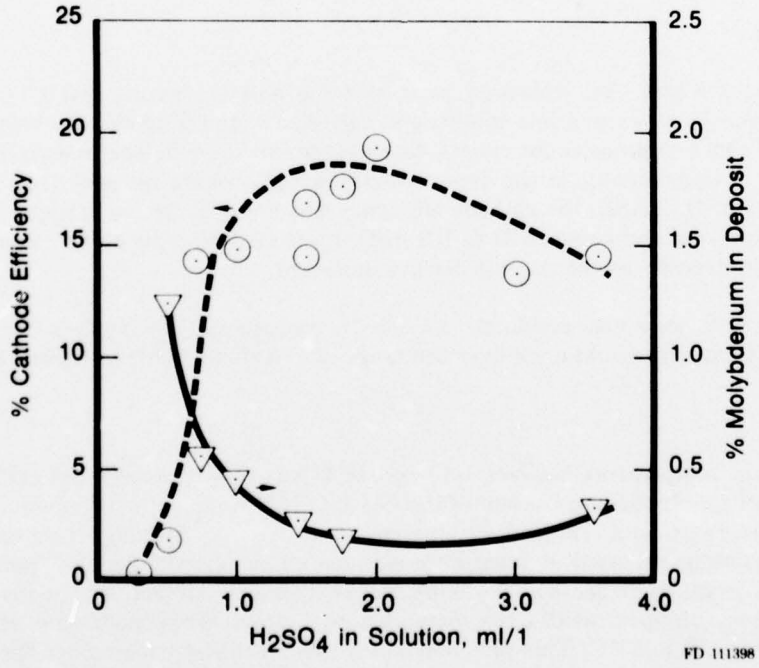

Figure 8. Effect of Catalyst on Cathode Efficiency and Molybdenum in Deposit

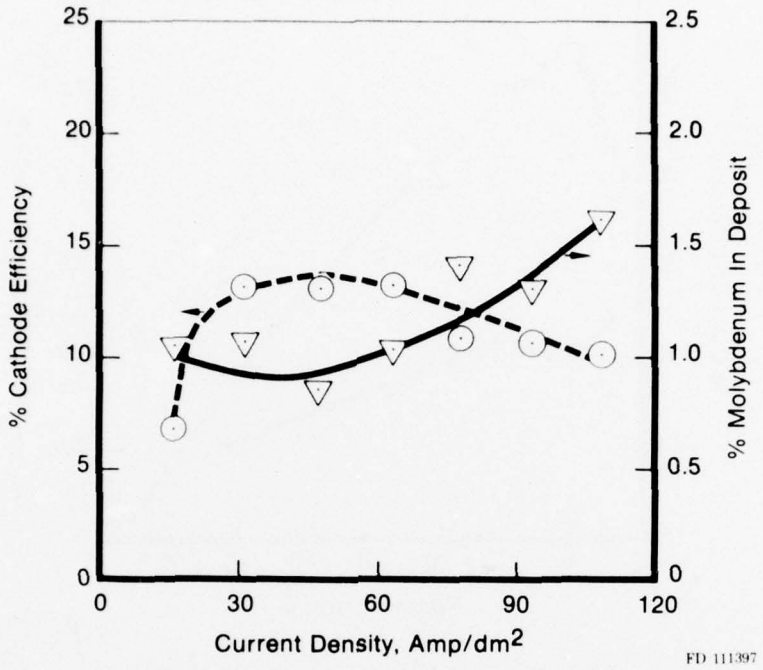

Figure 9. Effect of Current Density on Cathode Efficiency and Molybdenum in Deposits

TABLE 8. EFFECT OF CURRENT DENSITY ON CATHODE EFFICIENCY AND DEPOSIT COMPOSITION

Plating Solution: 300 g/l Self-Regulating Chromic Acid

75 g/l Ammonium Molybdate

Temperature: 47°C (117°F)

Sample Number	*Current Density, ASD (ASI)*	*Cathode Efficiency, %*	*Composition of Deposit, % Mo*
61	16 (1.0)	7.0	2.6
58	31 (2.0)	13.2	1.0
57	47 (3.0)	13.0	0.8
59	62 (4.0)	13.0	1.0
60	78 (5.0)	10.9	1.4
62	93 (6.0)	10.7	1.3
63	109 (7.0)	9.9	1.6

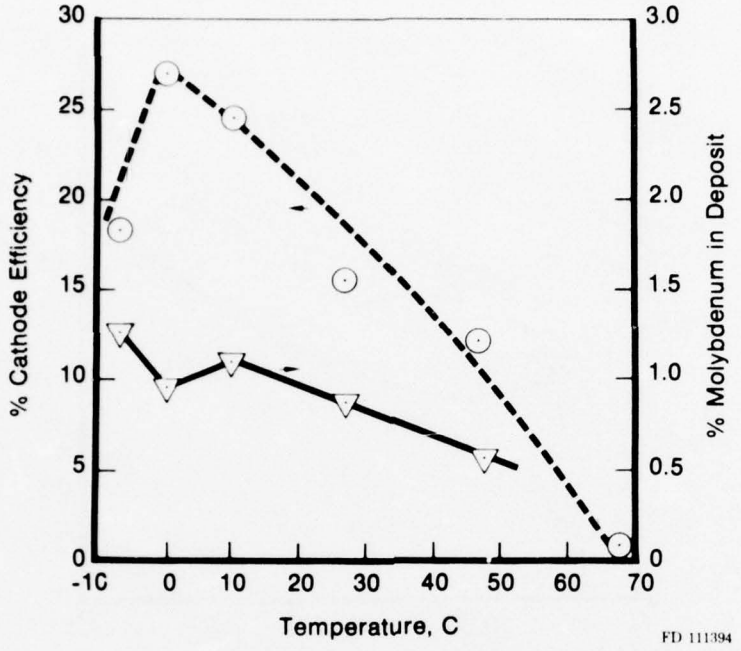

Figure 10. Effect of Temperature on Cathode Efficiency and Molybdenum in Deposit

TABLE 9. EFFECT OF TEMPERATURE ON CATHODE EFFICIENCY AND DEPOSIT COMPOSITION

Plating Solution: 300 g/l Self-Regulating Chromic Acid

75 g/l Ammonium Molybdate

Current Density: 47 ASD (3 ASI)

Sample Number	*Temperature, °C (°F)*	*Voltage, V*	*Cathode Efficiency, %*	*Composition of Deposit, % Mo*
167	10 (50)	5.4	24.6	1.1
168	10 (50)	5.3	23.7	1.7
169	27 (80)	5.0	15.2	0.9
170	66 (150)	4.6	0.1	-
171	- 8 (18)	6.4	18.3	1.2
172	0 (32)	5.8	27.0	0.9
175	27 (80)	5.2	20.8	1.1
177	27 (80)	5.1	17.7	0.9
42	49 (120)	5.0	12.8	0.6

Another factor which became evident from these studies is the effect temperature has on the adhesion and passivation of the titanium surface. At temperatures of −10°C the deposits were distinctly gray, while above 45°C local passivation of the surface, flaking of the deposits or dark areas on the surface resulted. From this and practical consideration of operating below room temperature, the preferred operating range of 35 to 40°C was established.

Alternating Current

To find ways to increase the concentration of molybdenum in the deposits, various cycles of current reversal and on-off cycling were evaluated using a periodic reverser.

When current reversing is used, the anodic dissolution occurs at close to 100% efficiency, so the anodic times had to be limited to no more than 10% of the cathodic times. Some deposits were obtained using this system and the amount of molybdenum increased by about 0.5% as compared to the uninterrupted DC plated samples. It took much longer to obtain sufficient deposits and this small increase in molybdenum content was not worth the longer times required to get the coatings. Larger increases without the longer times were possible using other methods.

A variation of current reversal using on-off cycling had more positive results and increases were generally on the order of 1% by simply pulsing the current in 0.5 to 1 second intervals. Using this technique in conjunction with an increased molybdenum content in the plating bath (95 g/l), deposits were obtained containing approximately 3% molybdenum. Cathode efficiencies of approximately 10% were maintained with this system.

The structure of deposits obtained with either alternating current or on-off current were fine grained and crack-free in appearance. These should therefore exhibit improved corrosion resistance as shown in Figure 11.

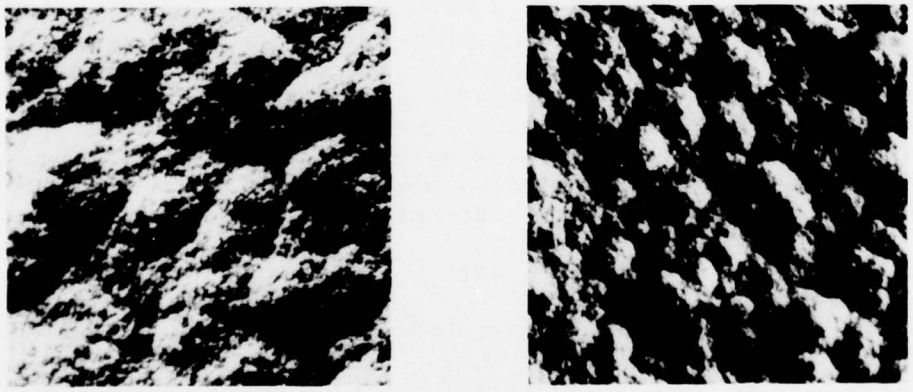

Chromium 1.5% Molybdenum Produced by Cycling Current On and Off

Chromium 1.5% Molybdenum Produced by Periodic Reversing Current

FD 111413

Figure 11. Scanning Electron Microscope Views at 1000X of As-Electroplated Chromium-Molybdenum Deposits

Hydrogen Pickup

Titanium alloys are severely embrittled by hydrogen absorption. Whenever exposed to a hydrogen-containing environment, they absorb hydrogen. During cathodic treatment in a chromic acid bath, approximately 90% of the total current is being used for generation of hydrogen. This part of the program was conducted to determine the extent of hydrogen pickup caused by the plating operation. As shown previously in Figure 2, the hydrogen content increased by 28 ppm after the conversion coating and by 68 ppm after plating. Apparently, the initial chromium-molybdenum surface layers retarded excessive absorption. After a diffusion heat treat, the hydrogen content is expected to significantly drop, but to minimize the possibility of damage between plating and diffusion, it is important that such contamination be limited. Subsequent analyses of similarly plated specimens made from either Ti 6Al-4V or Ti 8Al-1V-1Mo confirmed the hydrogen pickup occurring during plating is about 70 ppm, regardless of the titanium alloy.

Plating of stressed specimens loaded similar to the stress corrosion specimens discussed in a latter section of this report also confirmed that minimal hydrogen absorption takes place. After plating specimens with surface stresses above 689.5 MN/m² (100 ksi), no evidence of cracking of the Ti 8Al-1V-1Mo substrate could be detected either as plated or after removing from the constraining device and inspecting with fluorescent penetrants and chemical polishing as described in Reference 43.

Diffusion

Since both wear and corrosion occur as surface reactions, any type of protective coating must involve a change in the titanium alloy surface composition. The addition of both chromium and molybdenum to the surfaces forms an outer "skin" which provides a barrier between the titanium alloy and the surrounding environment.

It is possible to improve the adhesion of this coating by modifying the chemical composition of the titanium surface when the separate materials are diffused together by a suitable heat treat. This "surface alloying" modifies the chromium-molybdenum overlay so that it becomes an integral part of the titanium alloy component. The resulting dimensional change is less than the measured coating thickness, since at least part of the coating is made up of a diffused layer. The layer is easily seen by cross-sectional examination after etching with a Krolls solution composed of nitric and hydrofluoric acids. Microprobe analysis provides a better evaluation of actual diffusion depth of the alloying constituents into each other.

Mechanism of Coating Formation by Diffusion

Diffusion is a process whereby the distribution of each component in a phase tends to uniformity.

To reach a condition of equilibrium, the atoms must acquire sufficient energy to permit their displacement at an appreciable rate. The energy required to produce this displacement of chromium and molybdenum into titanium is provided by a rise in temperature of over 750°C.

Interdiffusion of chromium and titanium is generally accepted as being due to the motion of vacant sites within the lattice, solvent and solute atoms moving as the vacant sites migrate. The diffusion process is then dependent on the state of imperfection of both the titanium alloy and the surface alloy being formed.

Fick's equations express the depth of diffusion as a function of time and can be described by:

$$X^2 = 4\ kDt \tag{1}$$

where X is the depth of diffusion, k is a constant determined by the chromium concentration at the surface, D is the diffusion coefficient, and t is the time.

The diffusion coefficient varies with temperature according to the Arrhenius-type equation:

$$D = Do \exp(-Q/RT) \tag{2}$$

where T is the absolute temperature, R is the gas constant, Q the energy of activation and Do the diffusion factor.

Experimentally Determined Diffusion Coefficients

Diffusion coefficients for chromium from an electrodeposited alloy containing 1% molybdenum into three different titanium alloys were determined experimentally. The value of k in equation (1) was assumed equal to one. These results are summarized on Table 10 and typical microprobe photographs of cross sections used to measure diffusion depths are shown in Figures 12 through 14. The microprobe traces show the amount of chromium in the metal. The greater the separation in the two white lines, the greater the amount of chromium in the metal at the location of the line. Plotting the logarithm of D as a function of the reciprocal temperature, as shown in Figures 15 through 17, gives the expected straight line relationship from which activation energies for diffusion can be calculated from the slopes of the lines. Ti 8-1-1 had the highest activation energy (75.1 kcal) while Ti 6-6-2 had the lowest (47.2 kcal). The Ti 6-4 has an activation energy for diffusion between the two of 59.5 kcal. By combining equations (1) and (2) and using the experimentally determined constants, the depth of diffusion can be calculated for any given temperature/time combination for each of the three titanium alloys by using the formula:

$$X = [4\ t\ Do \exp(-Q/RT)]^{1/2} \tag{3}$$

where X is the diffusion depth in cm, t is the diffusion time in seconds, R is the gas constant, 1.98 cal/K mole, T is the diffusion temperature, and Do and Q are dependent on the alloys as follows:

for Ti 6-6-2

$Q = 47{,}200$
$Do = 0.610$

for Ti 6-4

$Q = 59{,}500$
$Do = 154$

and for Ti 8-1-1

$Q = 75{,}100$
$Do = 7.02 \times 10^4$

These numbers are all based on a least squares fit of the data generated in this study.

Laser Diffusion

Any bulk diffusion heat treatment of titanium alloys in a finish machined form and above 600°C can cause distortion. Treatment of coated alloys at temperatures above this point must, therefore, be done carefully, and may require some type of restraining device to maintain dimensions. This part of the investigation was undertaken to determine if laser heating can be used to diffuse the coating into the titanium without heating the bulk of the alloy. Such treatment results in diffusion without distortion. This type of treatment has been used to harden steel surfaces by localized melting. The rapidly quenched surface layers reportedly possess unique properties not otherwise attainable, due to the rapid cooling rates after laser exposure (Reference 41).

A 250 watt CO_2 laser was used to irradiate chromium-molybdenum plated Ti-6Al-4V alloy. In one instance the as-plated alloy was used, while in another instance black-nickel was used over the chromium-molybdenum coating to enhance energy coupling.

TABLE 10. DIFFUSION RATE DATA

Temperature, °C	*Time, hr.*	*Thickness, cm*	*D, cm²/sec*
	Ti 6Al-4V		
760	1	0.00066	3.0×10^{-11}
760	16	0.0025	2.8×10^{-11}
815	13	0.0071	2.7×10^{-10}
871	1	0.0018	2.2×10^{-10}
871	15	0.0122	6.9×10^{-10}
871	64	0.0178	3.0×10^{-10}
927	1	0.0066	3.0×10^{-9}
982	1	0.0076	4.0×10^{-9}
982	1	0.0091	5.8×10^{-9}
	Ti 6Al-6V-2Sn		
760	1	0.00089	1.0×10^{-10}
760	16	0.0033	4.7×10^{-11}
760	62	0.0066	4.9×10^{-11}
871	1	0.0025	4.5×10^{-10}
871	15	0.014	8.7×10^{-10}
927	1	0.0053	2.0×10^{-9}
927	15	0.015	9.8×10^{-10}
982	1	0.006	2.6×10^{-9}
982	1	0.007	3.5×10^{-9}
	Ti 8Al-1Mo-1V		
760	16	0.0013	7.2×10^{-12}
815	1	0.001	7.2×10^{-11}
815	13	0.003	5.8×10^{-11}
871	1	0.0018	2.2×10^{-10}
871	15	0.012	6.6×10^{-10}
871	64	0.020	4.5×10^{-10}
927	1	0.005	1.8×10^{-9}
927	15	0.015	9.8×10^{-10}
982	1	0.006	2.6×10^{-9}
982	1	0.010	7.2×10^{-9}

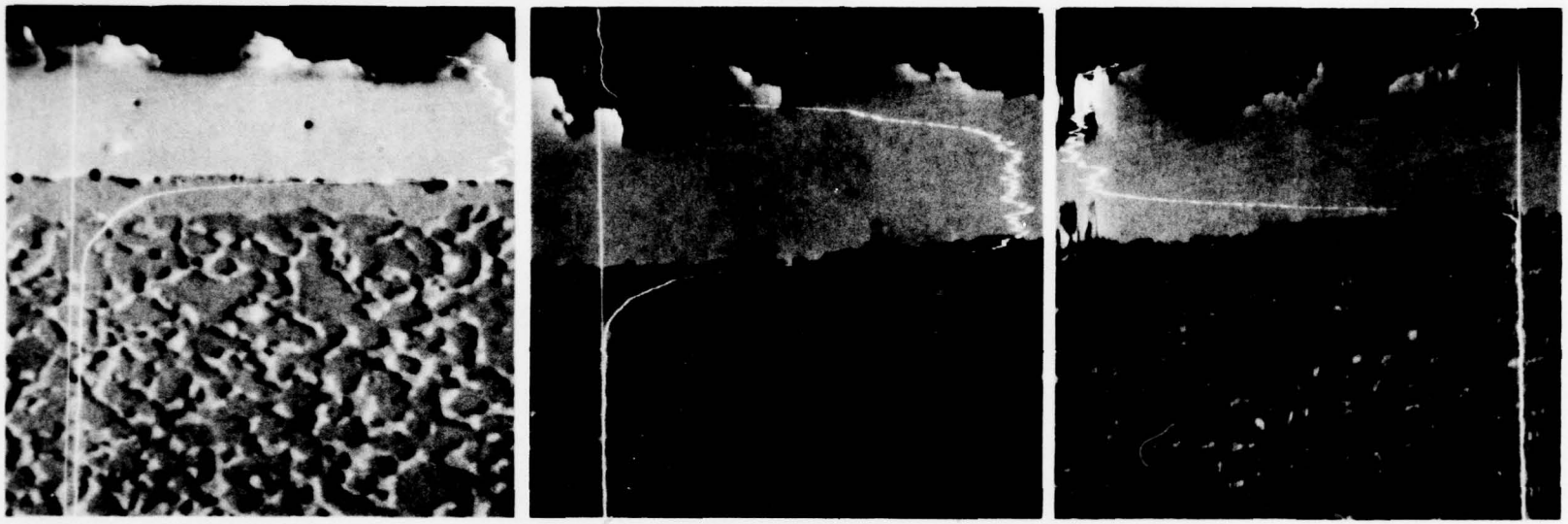

Ti 6Al-6V-2Sn

Ti 6Al-4V

Ti 8Al-1V-1Mo

Mag: 1000X

FD 113518

Figure 12. Microprobe Analysis of Chromium Diffusion Into Titanium Alloys After 1 Hour at 760°C

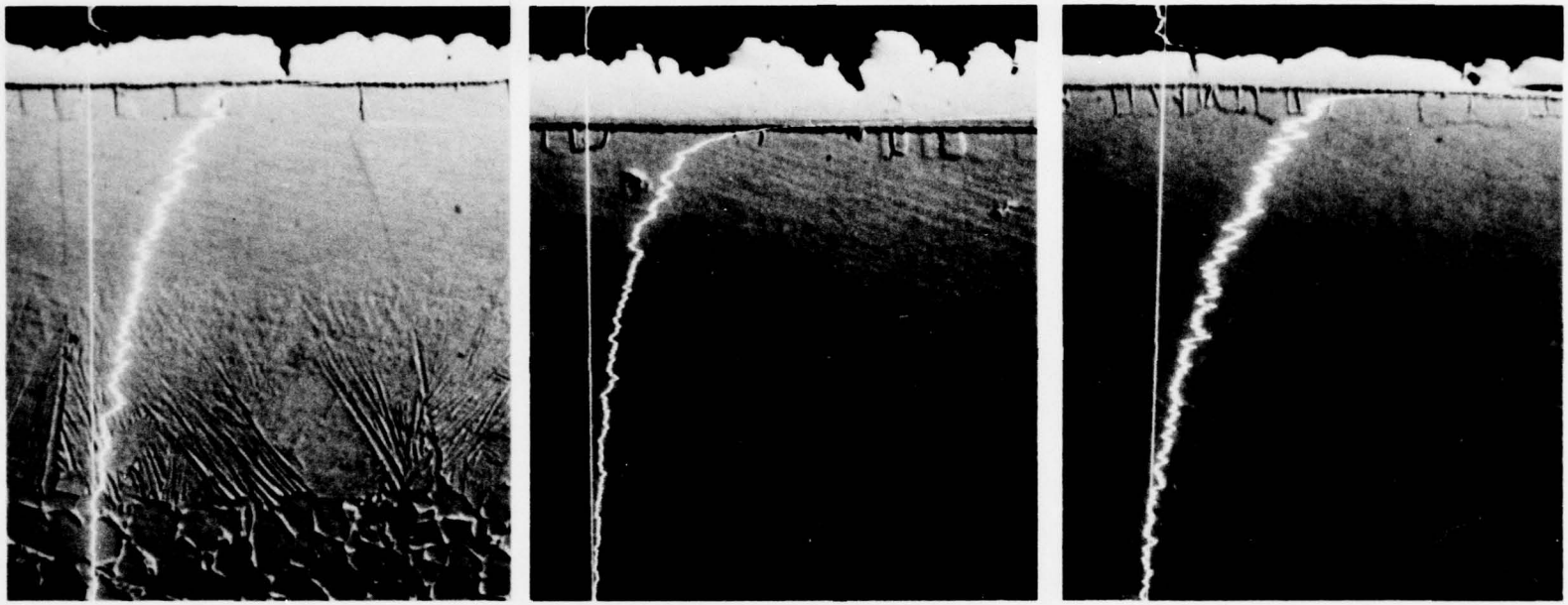

Figure 13. Microprobe Analysis of Chromium Diffusion Into Titanium Alloys After 15 Hours at 871°C

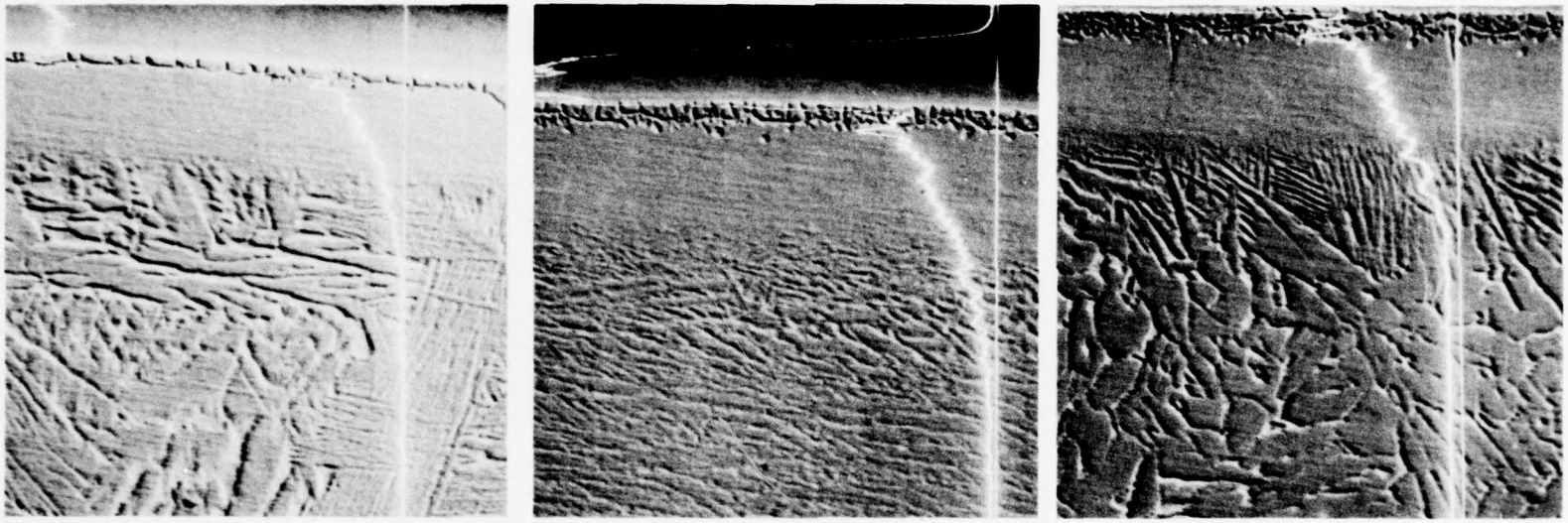

Figure 14. Microprobe Analysis of Chromium Diffusion Into Titanium Alloys After 1 Hour at 927°C

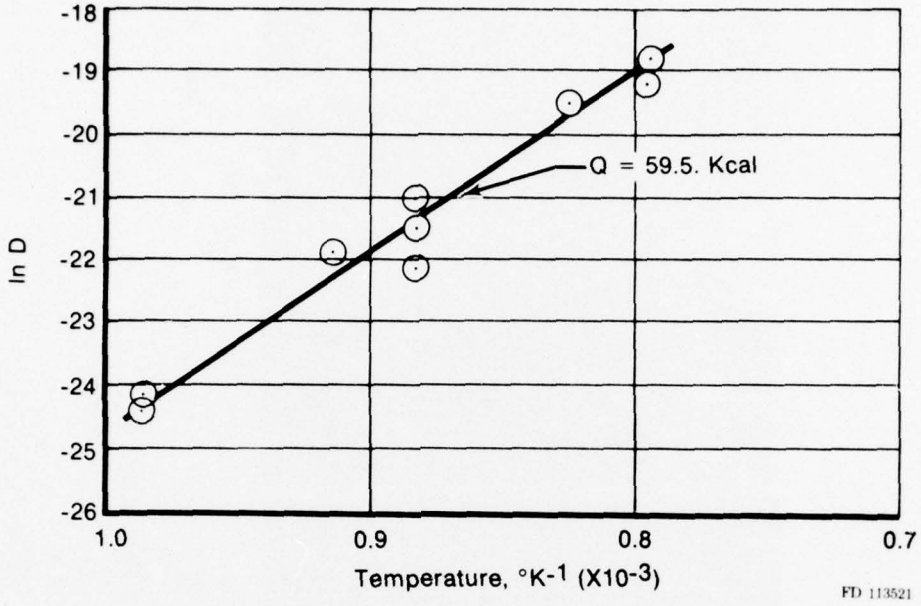

Figure 15. Arrhenius Plot for Diffusion of Chromium Into Ti 6Al-4V

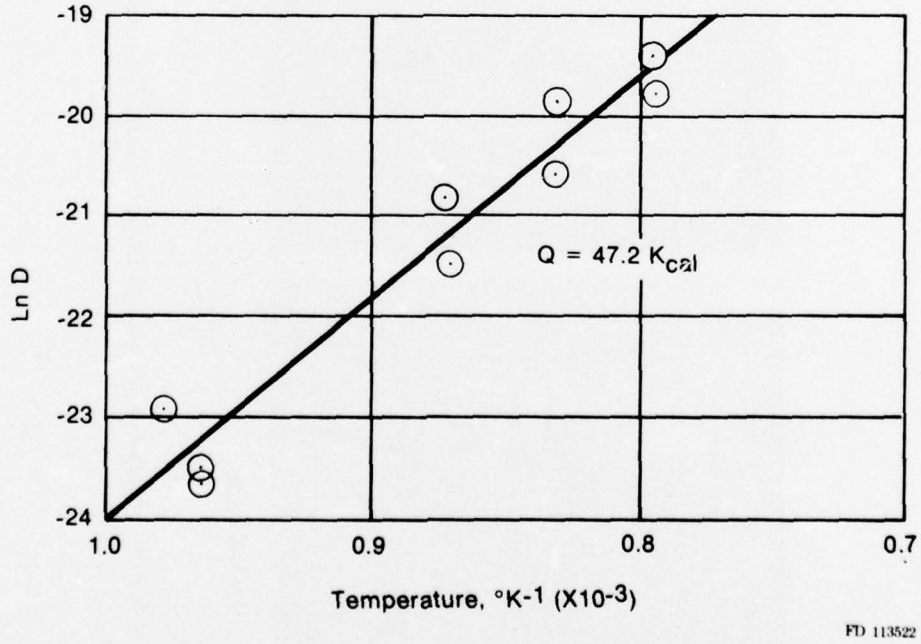

Figure 16. Arrhenius Plot for Diffusion of Chromium Into Ti 6Al-6V-2Sn

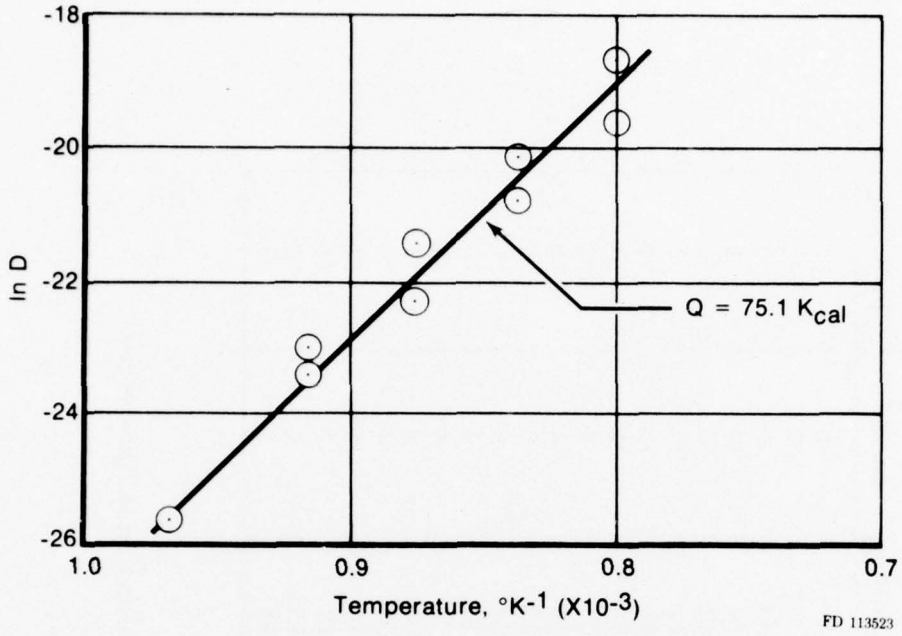

Figure 17. Arrhenius Plot for Diffusion of Chromium Into Ti 8Al-1Mo-1V

A matrix including several intensity/time combinations was evaluated on each of these alloys. The matrix and results are presented in Figures 18 and 19. Very little coupling of energy occurred on the chromium-molybdenum coated samples; however, the black-nickel did absorb the radiation and produced diffusion. Cross sections of the chromium-molybdenum plated sample showed no evidence of diffusion, even in the case of the highest power densities. Metallographic examination of the black-nickel coated samples will be completed in Phase II of this program.

Sputtered Coatings

High-rate triode sputtering was investigated as an alternate means of depositing chromium-molybdenum alloys. Sputtering has the advantage of depositing high molybdenum containing alloys. With plating, the upper limit of molybdenum attainable is about 3 wt %. The purpose of this investigation was to demonstrate that high molybdenum containing compositions can be deposited by sputtering and how deposition parameters affect structure. Two alloys were deposited by sputtering: a 95% Cr-5% Mo alloy and a 90% Cr-10% Mo alloy.

Experimental Procedure

Specimens (substrates) of Ti-6Al-4V alloy were coated in a two-target coater operated in the triode mode. The orientation of targets and substrate is shown in Figure 20. The substrates were rotated at 1/3 rpm. The targets were cast 95% Cr-5% Mo and 90% Cr-10% Mo alloys which were machined to 7.3 × 10.8 cm (2⅞ by 4¼ inches). Ground potential shields limited sputtering to a <6.7 × 9.2 cm (2⅝ by 3⅝-inch) area of each target. The sputtering chamber was pumped with a liquid nitrogen trapped 10.2 cm (4-inch) diffusion pump.

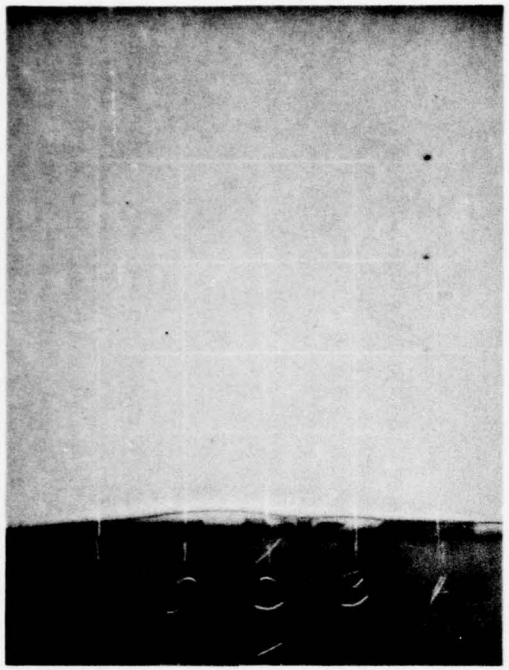

Location	Intensity, kw/cm^2	Time, sec
A1	16	20
A2	16	15
A3	16	10
A4	16	5
B1	12	20
B2	12	15
B3	12	10
B4	12	5
C1	8	20
C2	8	15
C3	8	10
C4	8	5
D1	4	20
D2	4	15
D3	4	10
D4	4	5
E1	1	20
E2	1	15
E3	1	10
E4	1	5

FD 113533

Figure 18. Effect of Laser Diffusion Treatment on Chromium-Molybdenum Coated Titanium Alloy

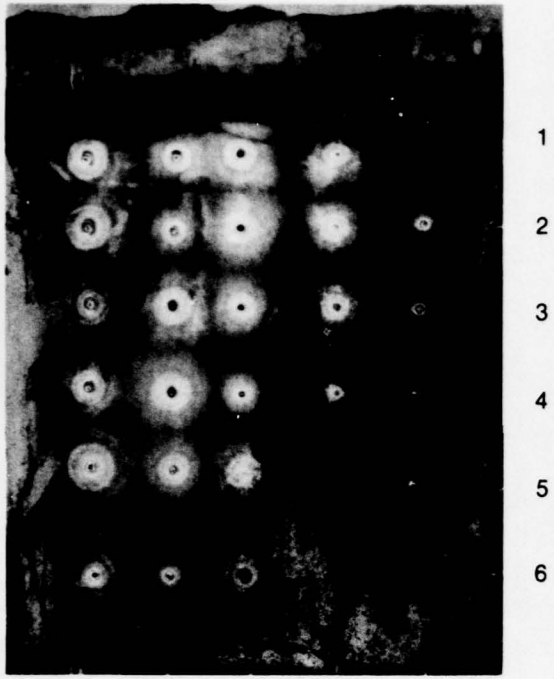

Location	Intensity, kw/cm^2	Time, sec
A1	12	15
A2	12	20
A3	16	5
A4	16	10
A5	16	15
A6	16	20
B1	8	5
B2	8	10
B3	8	15
B4	8	20
B5	12	5
B6	12	10
C1	1	15
C2	1	20
C3	4	5
C4	4	10
C5	4	15
C6	4	20
D1	-	-
D2	-	-
D3	1	1
D4	1	5
D5	1	10
D6	1	15
E1	-	-
E2	16	1
E3	12	1
E4	8	1
E5	4	1
E6	-	-

FD 113534

Figure 19. Effect of Laser Diffusion Treatment on Black-Nickel Coated Chromium-Molybdenum Coated Titanium Alloy

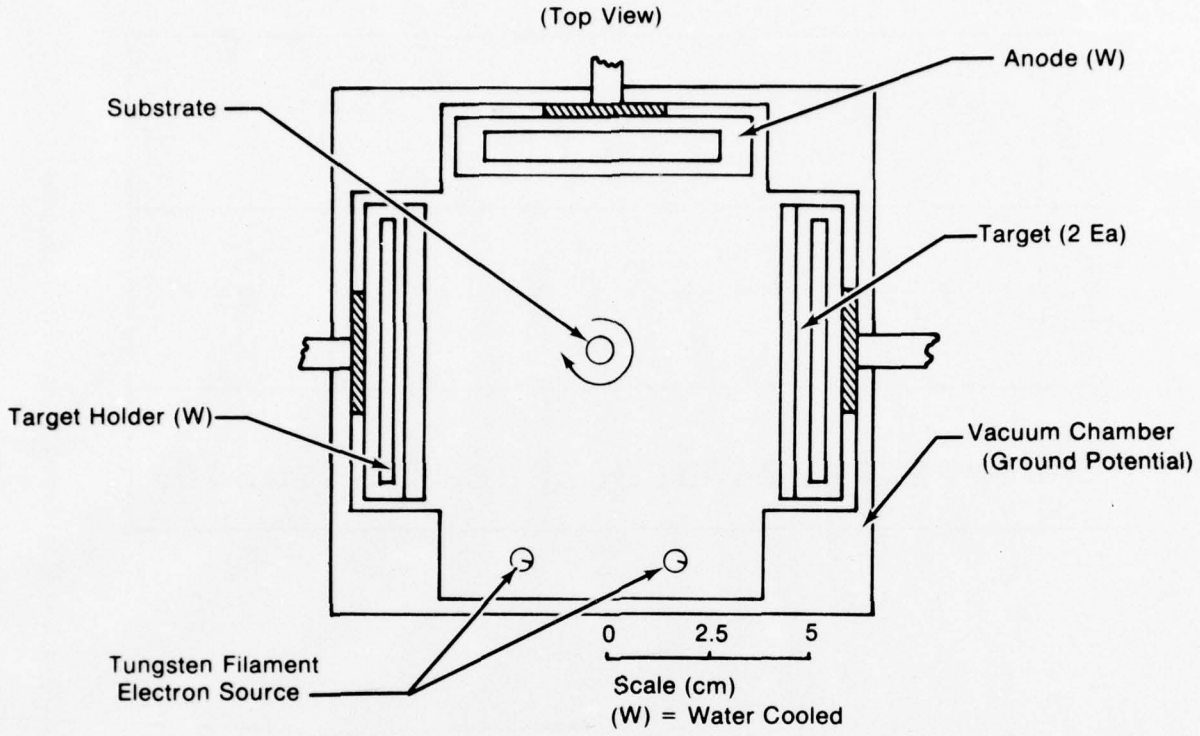

Figure 20. Schematic Coater (Some Ground Potential Shields Not Shown for Clarity)

Prior to insertion in the coater, all substrates were vapor blasted, scrubbed with scouring powder and rinsed with ethyl alcohol. Final cleaning in the system consisted of the following outgassing and sputter etching routine:

1. Radiation from the tungsten filaments was used to heat the substrate and other uncooled chamber parts. Heating was continued until chamber pressure was 4×10^{-7} torr or lower. The substrate temperature was estimated at 538°C (1000°F).*

2. The chamber was then backfilled to 3×10^{-3} torr with research grade krypton. A gas flow was maintained at this pressure by throttling the diffusion pump and regulating gas input to the system with a leak valve.

3. The triode discharge was established by applying a nominal 30 volts to the anode. A −25 volt bias was then applied to the substrate and targets for 5 minutes to facilitate outgassing.

4. The chamber was pumped to 4×10^{-7} torr and then again backfilled with krypton at 3×10^{-3} torr (flow).

5. A −50 volt bias was applied to substrate and targets for 30 minutes. Deposition was started by increasing the target voltage and decreasing the substrate bias to the desired levels. Deposition parameters are given in Table 12. Target current density was 4.6 ma/cm² ± 5% for all runs. Substrate

current densities increased with increasing negative bias voltage from 7.3 ma/cm² to 11.7 and 12.2 ma/cm² for 0V, −15V and −25V respectively. Target and substrate current densities were calculated by dividing the total electrode currents by their respective effective areas (area receiving ion bombardment). The krypton gas was kept at a pressure of 3×10^{-3} torr for all runs. Deposit thickness was determined from micrometer measurements made on the substrates before and after deposition. The temperature during each deposition was estimated at 816°C (1500°F)*.

Results

Metallographic data of the as-sputtered coatings are summarized in Table 11. The deposit thickness and corresponding diffusion zone depths were scaled from photomicrographs.

TABLE 11. SUMMARY OF SPUTTERED Cr-Mo COATINGS

Run No.	*Nominal Coating, mil*	*Nominal Diffused Zone, mil*	*Hardness, KHN*	*Composition, %Mo*
		95% Cr-5% Mo		
1	0.9	0.2	-	NM
2	1.2	3.1	-	NM
3	1.2	3.0	178	NM
4	1.0	2.4	-	NM
5	0.8	4.0	192	NM
6	1.6	0.9	-	NM
		90% Cr-10% Mo		
1	3.3	2.2	-	9.7
2	1.0	2.8	308	10.6
3	2.1	2.6	-	10.5
4	1.2	4.8	340	12.4
5	1.1	4.6	264	11.3
6	0.7	2.6	202	11.2

NM - Not Measured.

Where a 0V bias was used, the Cr-Mo structure was open, and typical of Zone I structures described by Movchan, et al, (Reference 42). However, the use of a negative bias (ion bombardment) resulted in complete densification. Photomicrographs in Figure 21 show the densification of structure at −25 volt bias for 90% Cr-10% Mo. These results are also typical for 95% Cr-5% Mo, Figure 22. The structures at −15V bias appear identical to the −25V bias structure, Figure 23. No variation in structure with target voltage was noted.

The 90% Cr-10% Mo sputtered deposits exhibited higher hardness than the 95% Cr-5% Mo deposits, Table 12. This effect was anticipated.

*Temperatures in similar experimental arrangements have been measured with a sheathed thermocouple, e.g., "Sputtered NiCrAlSi on TD-NiCrAl, Report of Processing History, Contract C-62220-C" 30 April 1975. R. J. Fenton and J. R. Mullaly. Prepared for NASA-LeRC.

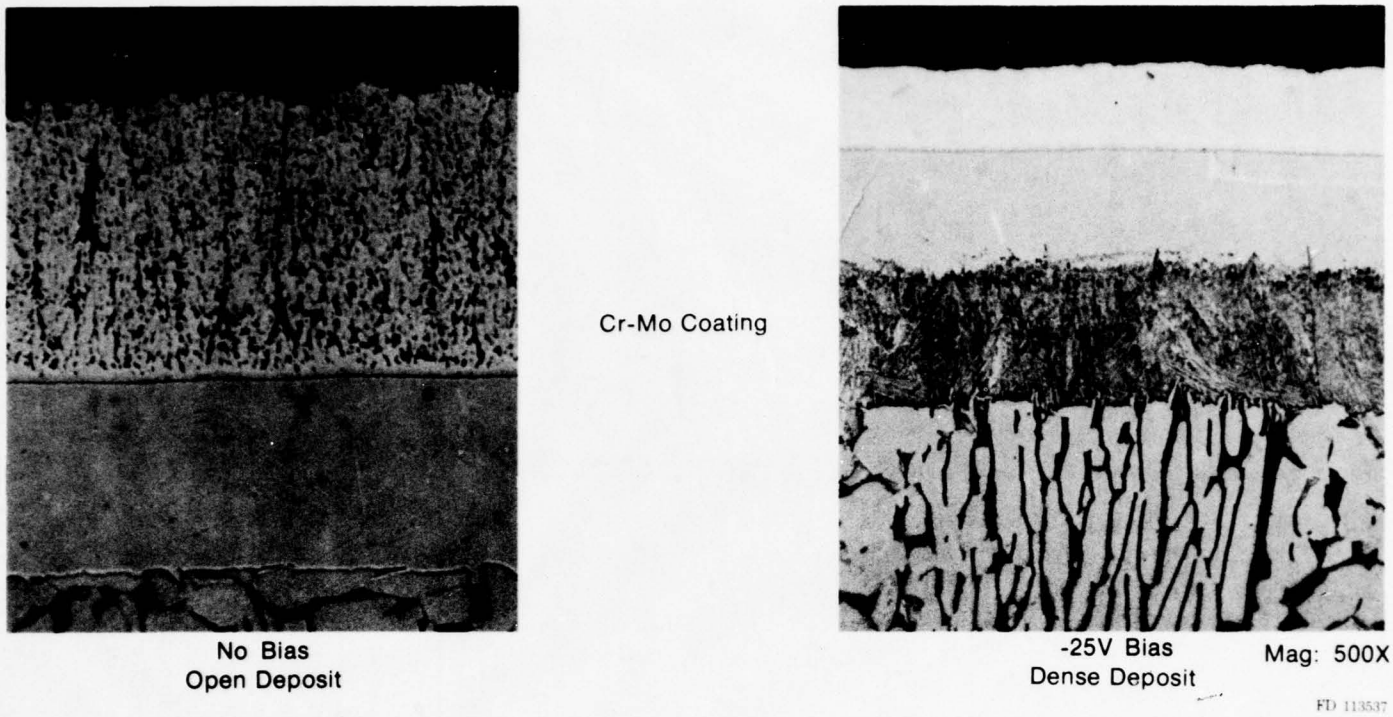

Figure 21. Effect of Ion Bombardment (Negative Bias) on Structure Refinement of 90% Cr-10% Mo Sputtered Coatings

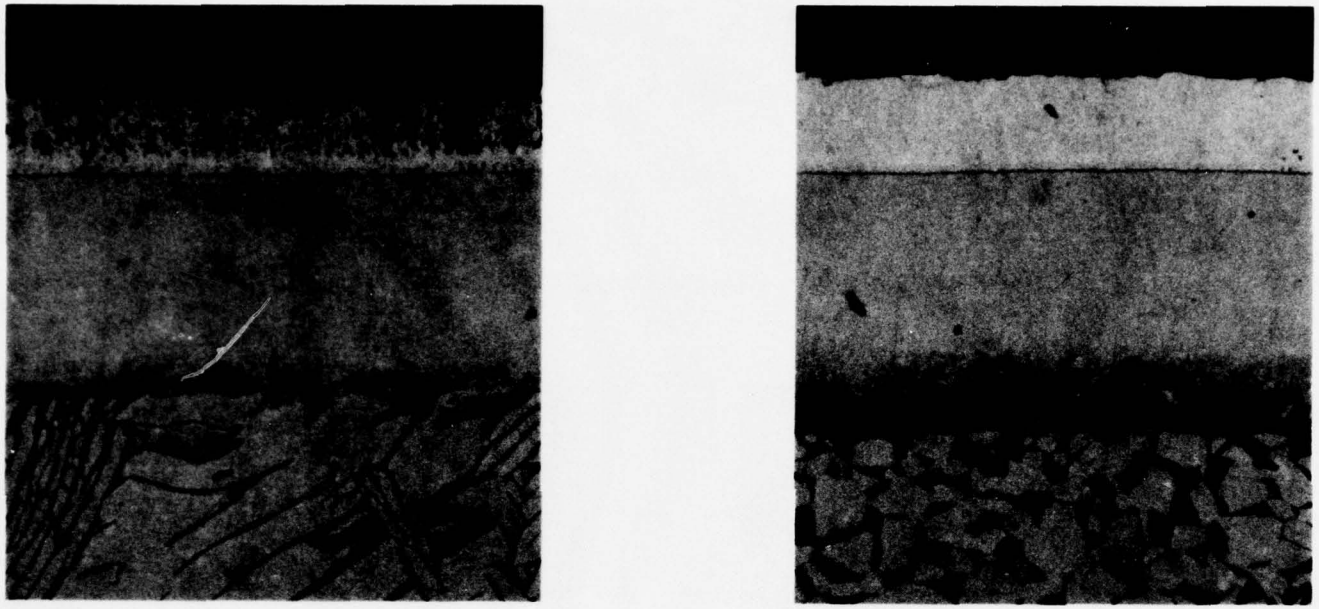

Figure 22. Effect of Ion Bombardment (Negative Bias) on Structure Refinement of 95% Cr-5% Mo Sputtered Coatings

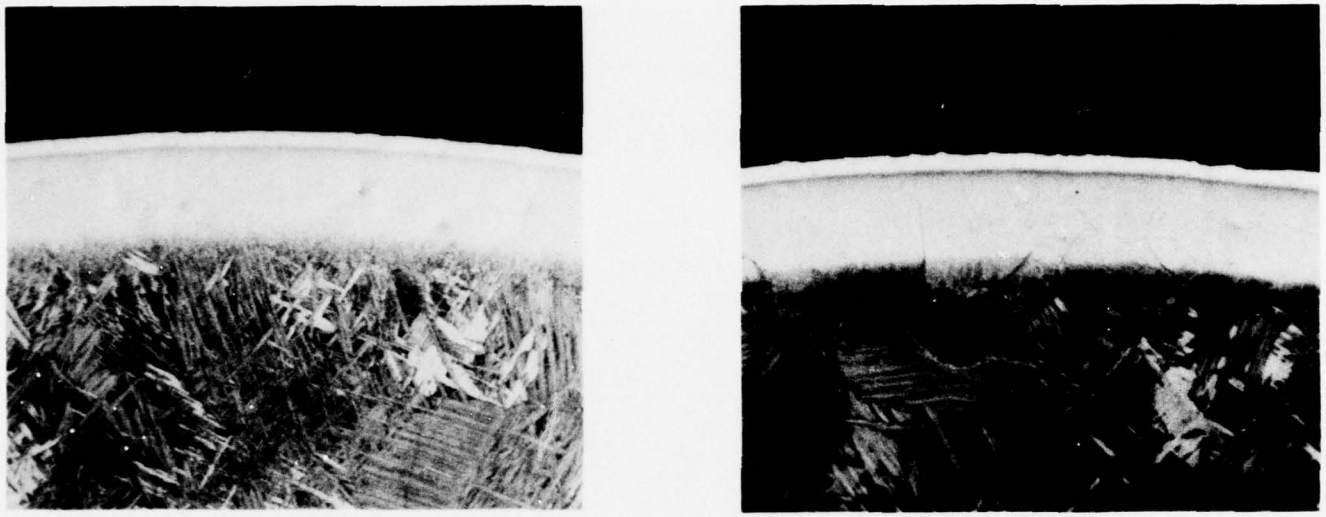

FD 113539

Figure 23. Dense 90% Cr-10% Mo Coatings Sputter Deposited With −15V and −25V Bias

TABLE 12. SUMMARY OF SPUTTERED Cr-Mo DEPOSITIONS

Run No.	Target, Volt	Substrate Bias, Volt	Deposition Time, hr	Deposition Rate, mil/hr
		95% Cr-5% Mo		
1	−500	0	6.0	0.15
2	−1000	−25	6.0	0.20
3	−1000	−15	5.5	0.22
4	−1000	0	5.25	0.19
5	−1500	−15	4.5	0.18
6	−1500	0	3.0	0.53
		90% Cr-10% Mo		
1	−1500	0	9.25	0.40
2	−1500	−25	4.3	0.22
3	−1500	0	5.0	0.42
4	−1500	−25	6.25	0.24
5	−1500	−15	5.5	0.20
6	−1000	−15	4.0	0.17

In summary, dense and adherent high molybdenum containing chromium alloy deposits can be obtained by sputtering. Further, the structure can be varied from open to dense by varying substrate bias voltage. Deposit thickness as well as interdiffusion bone thickness can be readily altered by varying deposition parameters.

ADHESION

Qualitative tests for electroplate adhesion are often satisfactory for quality control. Although no numerical values are obtained, these tests provide reliable indications of the degree of adhesion. The most satisfactory tests for a given electroplate are dictated by the type of deposit, the basis metal, and the intended application. The bend test was selected because it seemed most appropriate for the chromium-molybdenum deposit. This test allows evaluation of deposit adhesion under a gradation of induced stress. As the test piece is bent, it is subjected to varying amounts of stress. The proportion of adherent to nonadherent deposit and the location of the intact deposit both are qualitative indicators to coating integrity.

In our test, strips of Ti-6Al-4V; 2.54 by 1.27 by 0.05 cm (1 by 0.5 by 0.02 in.) were coated all over with chromium-molybdenum deposit. After appropriate diffusion heat treatment, they were bent over a 0.32 cm (0.125 in.) diameter mandrel. The appearance of the coating and underlying titanium substrate after bending was noted. Both sides of the strips (compressive and tensile stressed sides) were visually examined. Table 13 presents the results of the adhesion evaluation. As deposited, (no diffusion heat treatment) the coating tended to flake from both sides of the strip specimens.

All heat treatments improved the deposit adhesion so that only edge flaking occurred. When temperatures of 760°C or greater were used, the adhesion was sufficient to prevent flaking. However, at 815°C and above, several specimens were embrittled and broke when bent around the mandrel. Apparently, sufficient oxygen was picked up to reduce the ductility on those specimens heat treated in a slightly contaminated atmosphere. Uncoated titanium bend strips were subjected to the same heat treat and those too were embrittled. When special precautions were taken to reduce the oxygen contamination, the chromium-molybdenum coated specimens were not embrittled. Surprisingly, an uncoated specimen that was heat treated along with the coated specimen did break when bent around the mandrel (Figure 24). This indicates the chromium-molybdenum coating provides either some improved resistance to oxygen penetration or some improved tolerance to oxygen contamination.

TABLE 13. EFFECT OF DIFFUSION HEAT TREAT CYCLE ON COATING ADHESION

Diffusion Temperature, °C	*Time, hr*	*Results*
Not heat-treated	-	Flaked off from both sides
482	1	Flaked off from edges
538	1	Flaked off from edges
538	1	Flaked off from edges
760	1	No flaking
788	1	No flaking
815	1	Specimen fractured - Plate bonded
815 (Double Thick)	1	Specimen fractured - Plate bonded
* 815	1	Specimen fractured - Plate bonded
* 815 (No Plate)	1	Specimen fractured
* 815	1	No flaking
* 815 (No Plate)	1	Did not fracture
870	1	Specimen fractured - Plate bonded
870	1	Specimen fractured - Plate bonded
870	1	No flaking
* 870	1	No flaking - Did not fracture
* 870 (No Plate)	1	Specimen fractured
* 870/590	¼	Specimen fractured - Plate bonded
* 870/590 (No Plate)	¼	Specimen fractured
* 870/590	¼	Some flaking on compression side
* 870/590 (No Plate)	¼	Specimen fractured
870 (Peened)	1	Specimen fractured - Plate bonded

* These specimens were diffusion heat treated simultaneously.

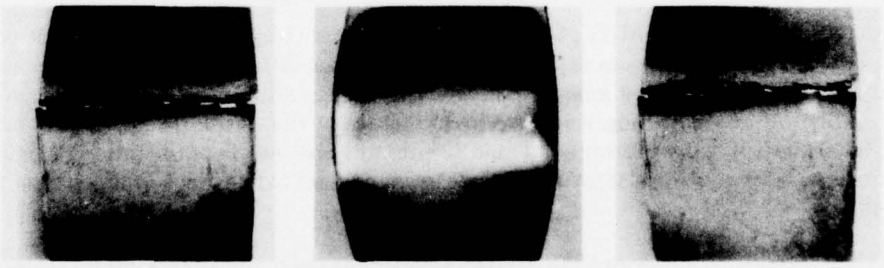

Figure 24. Oxygen Contamination Causes Embrittlement 870°C/1 hr

In order to prevent embrittlement, the diffusion cycle should then either be below 800°C or be conducted in a very "clean" atmosphere. Further, for maximum adhesion, temperatures should be above 700°C. The range of 700°C to 800°C provides satisfactory coatings. Temperatures in excess of 800°C may be useful in special cases where more diffusion is required and when suitable atmospheres can be assured.

HOT SALT STRESS CORROSION

A few of the essential features of current theories on hot-salt stress corrosion (HSSC) of titanium can be cited:

- In order for HSSC of titanium to occur, the environment must be characterized by a stressed condition, a high temperature, the presence of chloride ion, water, and probably some finite partial pressure of oxygen. The incidence of cracking appears to be quite sensitive to very slight changes of these elements.

- HSSC is observed as fine line cracking with sustained brittleness at the crack tip. This fine line cracking is in line with a corrosion which is concentrated at the tip.

- Crack propagation is fairly rapid and uniform. Average values for most metals have been measured at 0.5 cm/hr. This propagation rate is much faster than ordinary corrosion rates and too slow for brittle mechanical failure rates. It is reasonable for either electrochemical corrosion or alternating bursts of mechanical failure followed by slow corrosion.

- HSSC has two distinct phases: a crack incubation or induction period, and a crack propagation period. Since crack propagation has been observed to be rapid, the induction period represents the major portion of part life.

- All titanium alloys show a sensitivity in varying degrees to HSSC.

- The source of chloride, i.e., sea water, maintenance materials, does not appreciably affect the threshold stress for cracking.

Most of the proposed mechanisms rest on one or more of the above features. The literature contains reviews (References 21 through 36) which adequately cover the history of these mechanisms so will not be further discussed in this report.

Specimen Testing

The 1% molybdenum-chromium deposits were evaluated for hot-salt stress corrosion resistance with and without the diffusion cycles, using two-point loaded bent beam Ti 8Al-1V-1Mo specimens as described in detail in Appendix B.

Tests were conducted on AMS 4916 material machined into strips 0.089 by 1.25 by 15 cm. The length dimension was varied to produce the desired stress as calculated using the method described by Haaijer and Loginow (Reference 20).

Figure 25 shows the typical appearance of stress corrosion specimens mounted in the holder. After stripping the chromium-molybdenum coating in hydrochloric acid, the specimens were cleaned, chemically polished, and inspected for cracks using both visual and fluorescent penetrant techniques. Figure 26 shows the appearance of several specimens tested at 413.4 MN/m^2 (60 ksi). The cracks were readily visible after fluorescent penetrant processing when examined under ultraviolet light. Tables 14 and 15 summarize the results of these tests. Referring to Table 14 the uncoated alloy had, as expected, a threshold stress for cracking somewhere below 275.6 MN/m^2 (40 ksi). Plating this alloy with chromium-molybdenum improved the HSSC resistance so that the threshold stress was raised to above 413.4 MN/m^2 (60 ksi). After diffusing the coating at either 760°C (1400°F) or 870°C (1600°F), the threshold stress was again reduced to below 275.6 MN/m^2 (40 ksi). Glass bead peening (5N2) did not appear to affect the results of the specimens diffused at 760°C (1400°F), but did improve the threshold stress for specimens diffused at 870°C (1600°F).

Understanding these results depends on understanding that the ratio of undiffused coating thickness to diffused coating thickness is largest at the lower diffusion temperature. Therefore, the absolute thickness of pure or undiffused coating decreases as the diffusion temperature increases. The as-plated specimens demonstrated excellent resistance to penetration by chloride ions, hence, had good resistance to cracking. After diffusion at either 760°C or 870°C, a small amount of oxygen might have absorbed in the lattice, or a thinner undiffused coating on the surface after diffusion provided a path for chloride ions to reach titanium to start the cracking process. Peening normally improves the stress corrosion resistance by cold working the surface and producing compressive stresses. The specimen diffused at 760°C failed after peening, since the coating was still thick enough to prevent substantial compressive stresses from being induced into the titanium surface. Peening of specimens diffused at 870°C did put compressive stresses in the surface since the coating was thinner (more of it was diffused into the base alloy). The specimen did not fail.

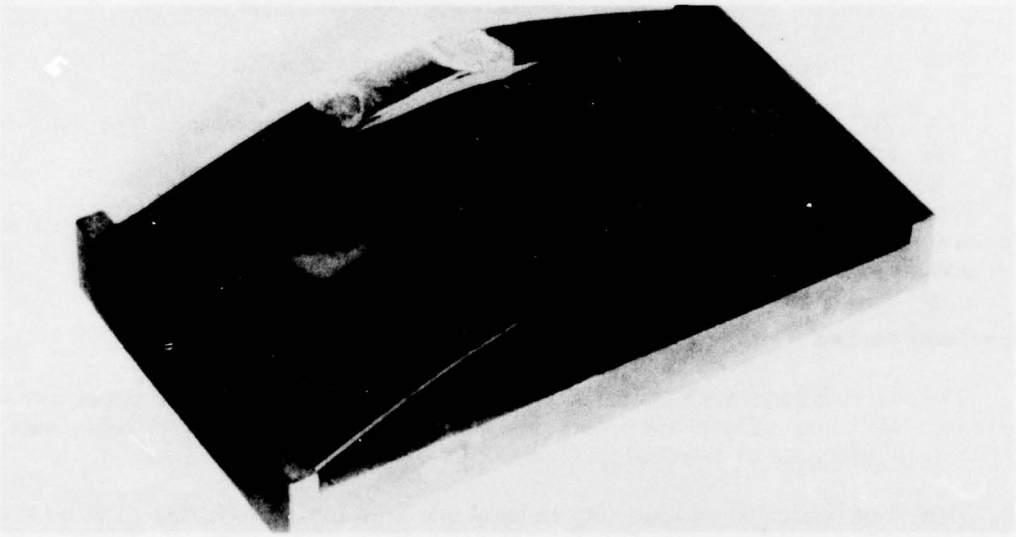

FE 153218A

Figure 25. Stress Corrosion Cracking Test Holder and Specimens

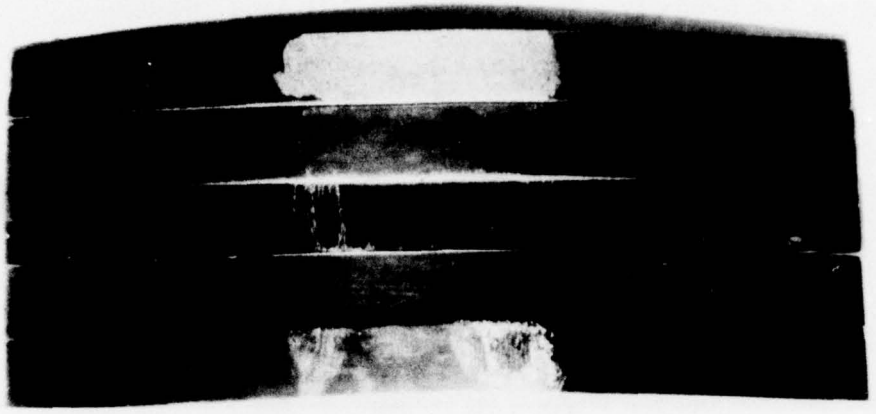

AV 111395

Figure 26. Appearance of Stress Corrosion Specimens After Testing

TABLE 14. HOT-SALT STRESS CORROSION TEST RESULTS ON CHROMIUM-MOLYBDENUM COATING

Base Material: Ti 8Al-1Mo-1V Sheet
Test Temperature: 480°C (900°F)
Contamination: 3% Aqueous Sodium Chloride
Time: 100-Hour

Sample Number	*Contamination*	*Stress, MN/m² (ksi)*		*Mo Content, %*	*Heat Treatment °C/hr*	*5N2 Glass Bead Peen*	*Results*
201	-	344.5	(50)	-	-	-	Pass
202	NaCl	344.5	(50)	-	-	-	Fail
203	NaCl	344.5	(50)	1	-	-	Pass
205	-	275.6	(40)	-	-	-	Pass
206	NaCl	275.6	(40)	-	-	-	Fail
207	-	275.6	(40)	1	-	-	Pass
208	NaCl	275.6	(40)	1	-	-	Pass
209	-	275.6	(40)	1	870/1	-	Pass
210	NaCl	275.6	(40)	1	870/1	-	Fail
211	-	275.6	(40)	1	870/1	Yes	Pass
214	-	344.5	(50)	1	-	-	Pass
215	-	344.5	(50)	1	760/1	Yes	Pass
216	-	344.5	(50)	1	870/1	Yes	Pass
217	-	344.5	(50)	1	870/1	Yes	Pass
219	NaCl	344.5	(50)	1	-	-	Pass
220	NaCl	344.5	(50)	1	760/1	Yes	Fail
221	NaCl	344.5	(50)	1	870/1	Yes	Pass
222	NaCl	344.5	(50)	1	870/1	-	Fail
223	-	413.4	(60)	-	-	-	Pass
224	-	413.4	(60)	1	-	-	Pass
225	-	413.4	(60)	1	760/1	Yes	Pass
226	-	413.4	(60)	1	870/1	Yes	Pass
227	-	413.4	(60)	1	870/1	-	Pass
228	NaCl	413.4	(60)	-	-	-	Fail
229	NaCl	413.4	(60)	1	-	-	Pass
230	NaCl	413.4	(60)	1	760/1	Yes	Fail
231	NaCl	413.4	(60)	1	870/1	Yes	Pass
232	NaCl	413.4	(60)	1	870/1	-	Fail

TABLE 15. SUMMARY OF HOT-SALT STRESS CORROSION TEST RESULTS ON SALTED AMS 4916

Temperature: 480°C

Time: 100 hour

Stress MN/m² (ksi)	*Uncoated*	*Cr-Mo*	*Cr-Mo 750°C/1-hr Peen*	*Cr-Mo 870°C/1-hr*	*Cr-Mo 870°C/1-hr Peen*
413.4 (60)	Fail	Pass	Fail	Fail	Pass
344.5 (50)	Fail	Pass	Fail	Fail	Pass
275.6 (40)	Fail	Pass		Fail	

Good protection from stress corrosion should be possible by some type of duplex coating. Further, a distinction can be made between the two suggested causes of reduced protection observed after heat treat, oxygen contamination or thinner coatings, by testing duplex coating with and without subsequent heat treat.

OXIDATION

Studies of the oxidation characteristics of pure titanium have been extensively conducted by Kofsted et al. (References 37 and 38). Ferguson (Reference 39) more recently reviewed the literature with respect to titanium alloys.

In his review, Kofsted indicates that the oxidation of pure titanium goes through three distinct mechanism changes in the temperature region. In the first region, below 570°F, the oxidation rate follows a logarithmic law, which has been interpreted as resulting when oxidation takes the form of film formation. Oxygen dissolution into the metal is negligible compared to the film growth.

In the second temperature region, between approximately 299°C (570°F) and 593°C (1100°F) the oxidation is observed as following a cubic law. Apparently, oxygen diffusion into the metal is comparable to the rate of film formation. The highest temperature region of interest here between approximately 543°C (1100°F) and 843°C (1550°F) is one where the oxidation rate is initially parabolic, followed by a linear rate. In this region, the interstitial diffusion of oxygen into the base metal increasingly dominates.

The oxidation of titanium alloys is similar in character to the pure metal (Reference 39). That is, at the more elevated temperature, interstitial solid solution diffusion of oxygen plays a major role in the oxidative process. Substitutional alloying agents, as the α stabilizers, aluminum, tin, zirconium, and the β stabilizers, silicon, vanadium, molybdenum, etc., vary the kinetics of oxidation. Shamblen and Redden (Reference 40) followed the internal surface embrittlement by microhardness measurements on several titanium alloys; among them Ti 8Al-1V-1Mo, as well as unalloyed titanium. In general, the depth of diffusion was proportional to the amount of substitutional alloying agents.

Coated Specimens Oxidation Rates

A Cahn Thermogravimetric Analysis (TGA) Unit was used to study the high temperature stability of chromium-molybdenum coated and uncoated AMS 4911 sheet. The coating was plated onto a 6 by 10 by 0.03 cm thick AMS 4911 to a thickness of approximately 0.001 cm. Coating diffusion was conducted at 815°C (1500°F) for 1 hour in vacuum and then the coating was 5N2 glass bead peened. Smaller sections (1 by 1 cm) were cut from this panel so that total weight did not exceed the 1 gram electrobalance maximum capacity. For comparison, an uncoated sheet of AMS 4911 was likewise peened and cut into similar sized sections.

Weight gains were individually monitored using a recording electrobalance for approximately 24 hours. The results are summarized in Table 16 and Figures 27 and 28.

Oxidation rates at 500°C (932°F) did not seem to depend on whether the specimens were coated or uncoated. In both cases, the rates were low and should therefore not cause any detrimental effects. At 600°C, the differences between coated and uncoated specimens became more evident. The Cr-Mo coated pieces were still oxidizing at close to the rates shown for 500°C (1112°F), while uncoated titanium oxidized at a much greater rate. Raising the temperature to 700°C (1292°F) showed an even larger separation between coated and uncoated titanium. The coating was shown to improve the oxidation resistance at those temperatures.

These results demonstrate an improved oxidative stability of chromium-molybdenum coated titanium over the uncoated alloys. It appears the useful temperature range may be extended by about 100°C (200°F) when only oxidation limits the application temperatures.

TABLE 16. OXIDATION OF AMS 4911 WITH AND WITHOUT CHROMIUM-MOLYBDENUM COATING

Coating	*Sample Weight, mg*	*Temperature, °C (°F)*	*Time, minutes*	*Weight Gain, mg/sq cm*	*Absolute Rate of Wt. Gain, mg/sq cm/min*
No	116.4	700 (1292)	25	7.587×10^{1}	3.035×10^{0}
			79	2.265×10^{2}	2.867×10^{0}
			166	3.321×10^{2}	2.001×10^{0}
			307	5.045×10^{2}	1.643×10^{0}
Yes	129.2	700 (1292)	77	2.463×10^{1}	3.198×10^{-1}
			177	5.112×10^{1}	2.888×10^{-1}
			277	7.660×10^{1}	2.765×10^{-1}
			399	1.041×10^{2}	2.609×10^{-1}
No	117.3	600 (1112)	54	4.368×10^{-2}	8.089×10^{-4}
			344	1.626×10^{-1}	4.726×10^{-4}
			597	2.439×10^{-1}	4.085×10^{-4}
			914	2.997×10^{-1}	3.279×10^{-4}
			1,282	4.562×10^{-1}	3.559×10^{-4}
Yes	131.1	600 (1112)	266	1.133×10^{-2}	4.260×10^{-5}
			748	8.498×10^{-2}	1.136×10^{-4}
			1,381	1.813×10^{-1}	1.313×10^{-4}
No	101.9	500 (932)	240	1.076×10^{-2}	4.485×10^{-5}
			360	2.272×10^{-2}	6.312×10^{-5}
			540	4.904×10^{-2}	9.081×10^{-5}
			780	7.296×10^{-2}	9.353×10^{-5}
			900	8.492×10^{-2}	9.435×10^{-5}
			1,130	1.100×10^{-1}	9.737×10^{-5}
Yes	122.5	500 (932)	90	7.606×10^{-3}	8.451×10^{-5}
			210	1.648×10^{-2}	7.847×10^{-5}
			330	2.535×10^{-2}	7.683×10^{-5}
			510	4.310×10^{-2}	8.451×10^{-5}
			690	6.338×10^{-2}	9.186×10^{-5}
			1,404	1.014×10^{-1}	7.223×10^{-5}

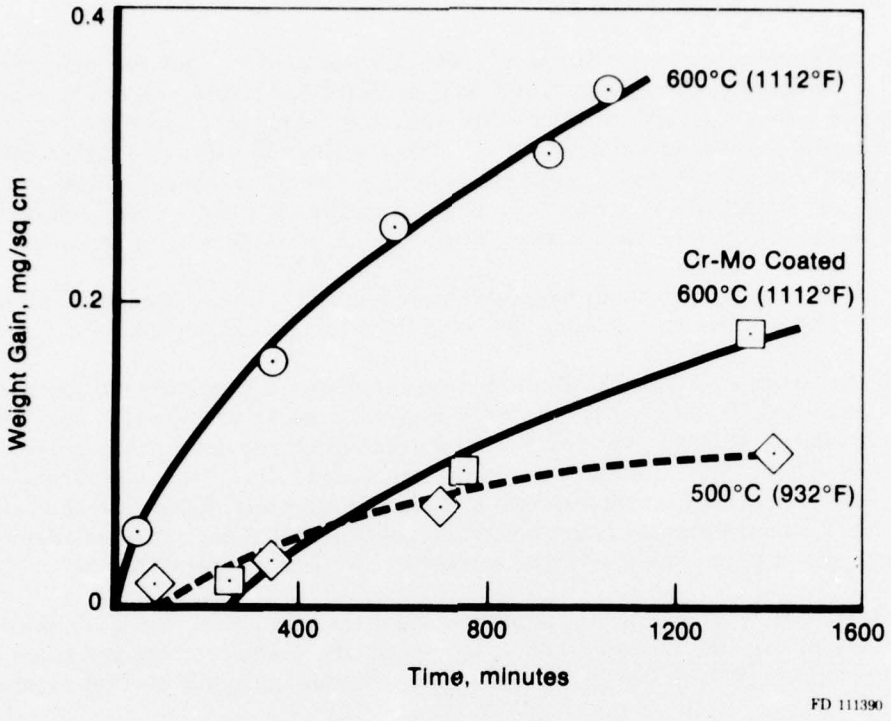

Figure 27. Oxidation Rate of Coated and Uncoated Ti 6Al-4V

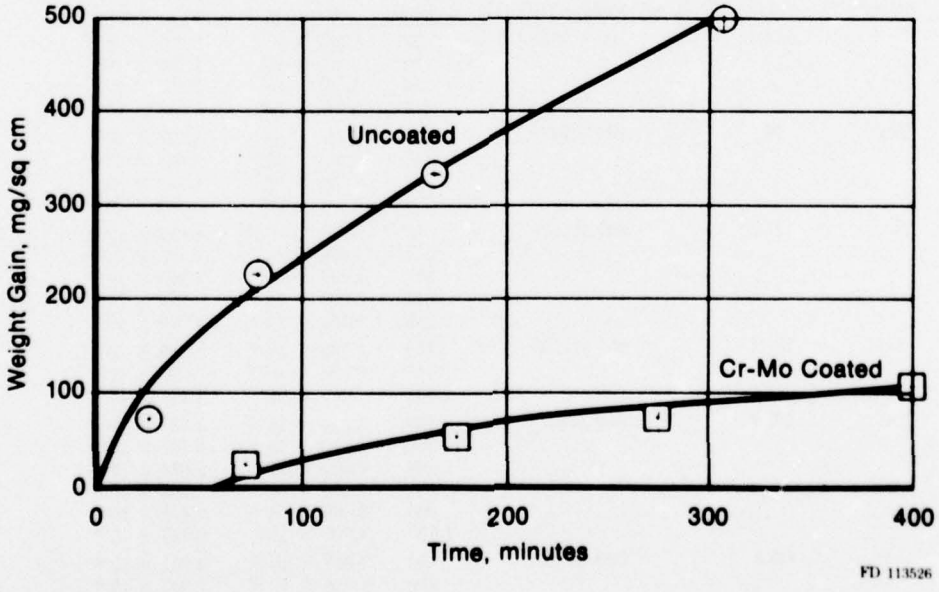

Figure 28. Oxidation of Coated and Uncoated Ti 6Al-4V at 700°C (1292°F)

WEAR RESISTANCE

The chromium-molybdenum coatings were evaluated for wear and frictional properties on a Falex wear testing machine. This equipment has received universal acceptance as a method for screening wear couples. While results are not always correlatable to in-service conditions, it does provide a somewhat controlled method of materials comparison in providing fixed specimen geometry.

The Falex wear testing machine is shown in Figures 29 and 30. A 0.635-cm diameter journal (pin) is rotated against two stationary V-blocks to give a four-line contact. The test pieces and their supporting jaws are immersed in the oil sample cup or run dry. Coatings or dry film lubricants to be investigated reside on pins and/or V-blocks. The pin is rotated at 290 rpm and a load is applied to the V-blocks through a nut-cracker action lever arm and spring gauge. The load is applied by means of a ratchet wheel mechanism that also may be used to indicate wear like a micrometer. An 18-tooth advance on the ratchet wheel is equal to 0.00254 cm of wear. The entire load arm assembly is free to rotate about the main shaft, and friction developed during the test is shown in inch-pounds on the torque gauge.

In the test method selected, the V-block load was increased incrementally according to the schedule given in ASTM-D-2625 Procedure A. It consists of running two stationary V-block specimens against a rotating pin until a sharp increase of 1.13 Nm (10 in.-lb_f) in steady-state torque or pin breakage is experienced. A prescribed schedule of jaw load application and dwell time on the rotating pin is followed: 3 minutes at 1300 N plus 1 minute at 2220 N plus 1 minute at 3330 N plus 4450 N until failure. Run-out time at the 4450 N level was set at 30 minutes.

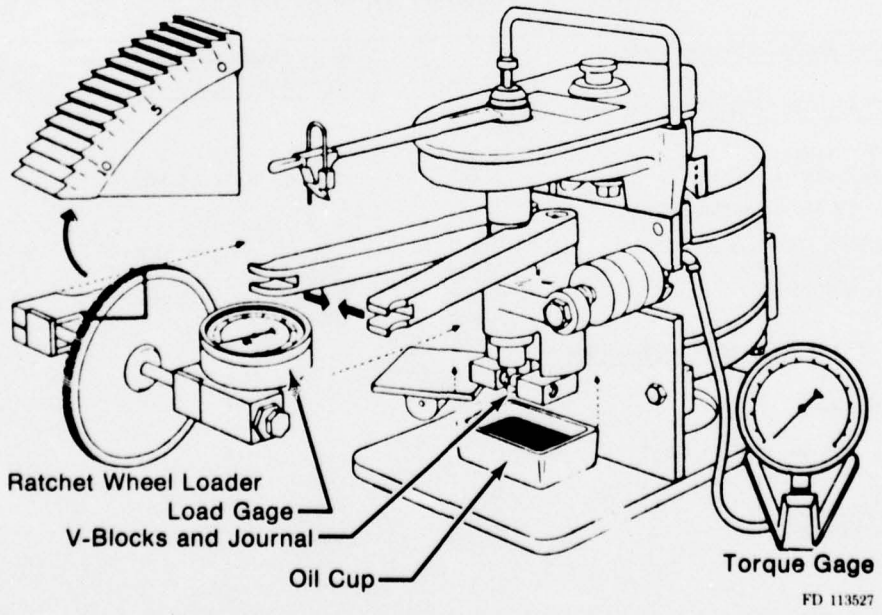

Figure 29. Schematic Diagram of Falex Lubricant Tester

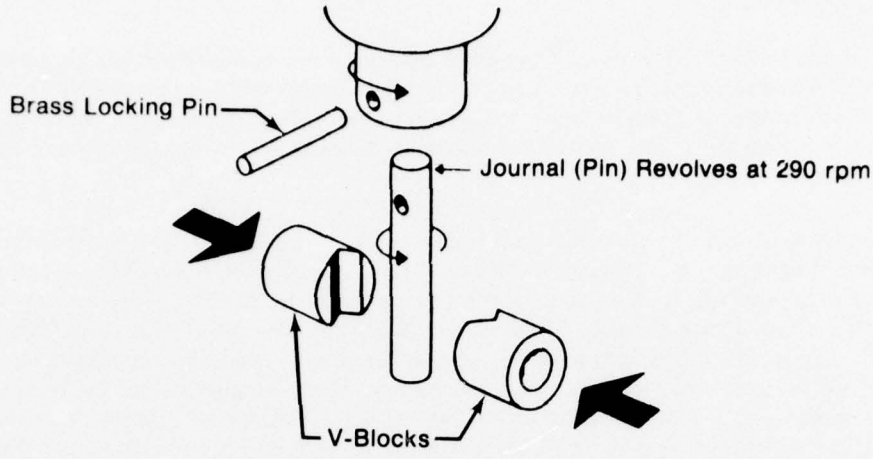

Figure 30. Exploded View of V-Blocks and Journal Arrangement, Falex Lubricant Tester

The pins used in this evaluation were Ti-6Al-4V; the V-blocks were either Ti-6Al-4V or AISI 1137 steel. MIL-L-23699 aircraft turbine engine lubricant was used where lubricant was specified.

The test results are compiled in Tables 17 and 18. In most instances, the titanium alloy blocks were coated with a 1% molybdenum coating although some were tested as-received (uncoated).

TABLE 17. FALEX WEAR TEST IN AIR

Test Material Combination[1]	*Time To Failure At Specified Load*			
	1330N (300 lbf)	*2220N (500 lbf)*	*3330N (750 lbf)*	*4450N (1000 lbf)*
STEEL V-BLOCKS/Titanium Pins				
1. Bare Titanium	3 min.	Failed		
2. Lube B Coated Titanium	3 min.	1 min.	1 min.	12 min.
1% Mo-Cr/760C-3 hr With				
3. Vapor Blast (VB)/Lube B	3 min.	1 min.	1 min.	8 min.
4. Duplex-VB/Lube A	3 min.	Failed		
5. Duplex-VB/Lube B	3 min.	1 min.	1 min.	20 min.
6. As plated	3 min.	Failed		
TITANIUM V-BLOCK/Titanium Pins				
7. Bare Titanium	½ min.			
8. Lube B (2)	½ min.			
1% Mo/870C-1 hr With				
9. Peened	1 min.			
10. Peened/Lube B	1 min.			
11. Peened/Lube B	3 min.	Failed		

Notes:

1. Failed indicates samples failed while the jaw load was being increased from one level to that level where Failed appears.
2. "Duplex" refers to two coating cycles being conducted on the part. After the initial coating was applied, the surfaces were vapor blasted and replated/diffused as with the first cycle.
3. Treatment refers to pins only.

TABLE 18. FALEX WEAR TEST USING MIL-L-23369 OIL

Test Material Combination[3]	*Time To failure At Specified Load*			
	1330N (300 lbf)	*2220N (500 lbf)*	*3330N (750 lbf)*	*4450 N (1000 lbf)*
STEEL V-BLOCKS/Titanium Pins				
1. Bare Titanium 6 to 4	3 min. 30 sec.	Failed[1]		
	3 min.	Failed		
1% Mo-Cr/760C-3 hr with				
2. Vapor Blasted	3 min.	1	1	30 min.
3. Peened	3 min.	1	1	30 min.
4. Duplex-Peened	3 min.	1	1	30 min.
1% Mo-Cr/870C-1 hr with				
5. As Plated	3 min.	1	1	0.5 min.
3% Mo-Cr/760C-3 hr with				
6. Vapor Blast	3 min.	1	1	2.5 min.
7. Peened	3 min.	1	1	12.5 min.
8. Duplex Peened	3 min.	1	1	30 min.
TITANIUM V-BLOCKS (1% Mo-Cr/760C-3 hr)/Titanium Pins				
1% Mo-Cr/760C-3 hr with				
9. Peened	3 min.	Failed		
10. Peened	3 min.	Failed		
11. Vapor Blast	3 min.	Failed		
3% Mo-Cr/760C-3 hr with				
12. Peened	3 min.	Failed		
13. Peened[2]	3 min.	Failed		

Notes:

1. Failed indicates samples failed while the jaw load was being increased from one level to the next higher.
2. Bare titanium.
3. Treatment refers to pins only.

Wear Test Results (Air)

As expected, bare titanium did not fare as well against itself as it did against steel. Chromium-molybdenum alone did not substantially improve the wear resistance unless it was used in conjunction with a dry film lubricant. The dry film lubricants evaluated were both synergistic combinations of molybdenum disulfide and antimony trioxide. In the case of Lube A a silicone binder is used which makes it susceptible to fuel and/or oil degradation. The Lube B material uses a thermosetting resin binder which is not affected by hydrocarbons.

Lube B did significantly improve the wear life of the titanium alloy against steel. When applied over a duplex coated chromium-molybdenum coating, the wear life was further improved.

All of the results generated using titanium alloy V-blocks, even with the dry film lubricants, showed much shorter lives than previous tests. Since P&WA is presently using chromium-molybdenum coating against itself and with Lube B in a highly loaded spherical bearing, the results obtained with this combination in Falex testing are difficult to understand. Tests using

titanium V-blocks with Lube B coating against steel pins showed similar short lives. Apparently the stationary line contact loading characteristic with V-blocks is significantly different from the sweeping line contact against the pins. Therefore, a somewhat modified loading cycle or test must be conducted on these combinations in order to get suitable results.

Wear Test Results (MIL-L-23369 Oil)

Bare titanium against steel failed this test, sometimes before completing the 3 minutes at the lowest load level. All of the chromium-molybdenum coating systems seemed to substantially improve the wear life although 1% Mo-Cr with a 3-hour 760°C diffusion cycle generally appeared better than either the 3% molybdenum coating or the higher diffusion temperature treated specimens.

Figure 31 shows the appearance of the specimens after testing. The specimens in that figure were selected to illustrate the vast improvement in wear life possible with the chromium-molybdenum coating on titanium.

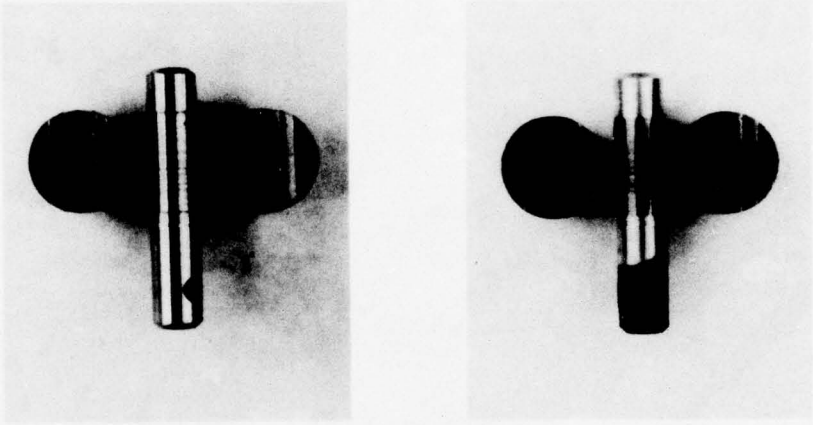

Figure 31. Comparison of Bare vs Chromium-Molybdenum Coated Ti 6Al-4V Pins Wearing Against Steel

As with the air tests, chromium-molybdenum coating life against steel V-blocks was markedly better than when tested against titanium V-blocks even though the V-blocks were chromium-molybdenum coated. This is again explained by the test configuration and loading sequence just not allowing valid testing of this material combination.

EROSION RESISTANCE

The ability of aircraft components to withstand erosion by airborne particles, such as sand or dust, often bears a direct relationship to performance and life. For this study, 1% and 3% chromium-molybdenum coatings were applied to 8 by 8 by 0.25 cm specimens of Ti 8Al-1V-1Mo alloy. These coated specimens, along with uncoated specimens, were impinged by a high-velocity stream of 27 micron aluminum oxide particles. Each test piece had sufficient surface area to

permit several test runs. An SS White Model F Industrial Airbrasive Unit generated the impinging particles as illustrated in Figure 32. In this rig, small diameter abrasive particles are metered into a gas stream. The abrasive is contained in a vibrating reservoir. At constant gas pressure, the amount of abrasive metered into the stream is a function of the vibrating intensity of the reservoir. Solenoid operated valves allow accurate control of gas/ abrasive flow necessary for reproducible results with short dwell test piece exposures. Abrasive flowrate through the 0.066 cm (0.026 inch) diameter orifice nozzle was 0.52g/min when the propellant gas (nitrogen) pressure was set at 0.688 MPa (100 psig). Flowrate, nozzle diameter, and gas pressure remained constant during the test series. Each site was impinged for 10 seconds at either of two impingement angles: 20 deg and 90 deg relative to the plane of the coated surface.

Several means of determining or characterizing erosion resistance were considered. The most commonly used is weight loss; however, when coatings are not the same density or do not possess a constant density across their effective thickness (such as diffused coatings), weight loss can be misleading. Volume loss by direct measurement was not possible experimentally, nor was calculated volume loss which depends on an accurate determination of coating density. In this effort, we chose to assess erosion by tracing the erosion site with a surface profilometer. This method provides a two-dimensional view of the site from which erosion depth can be read directly (Figure 33).

A Gould Model 156 Surfanalyzer surface profilometer was used to measure the depth of erosion after each test. The results of these tests are summarized in Table 19, along with the erosion depth measurements.

At the 20-deg impingement angle, all of the coating compositions and diffusion cycles reduced the erosion rate to approximately half that of the uncoated alloys. At the 90-deg impingement angle, although the erosion rates were generally greater, the coated samples again exhibited only half the erosion rate of uncoated samples.

These results demonstrate that the chromium-molybdenum coating on titanium alloys offers substantial erosion protection to these alloys.

HIGH-FREQUENCY FATIGUE

For many applications of coated titanium alloys, it is important that the coating not compromise mechanical properties. Earlier testing of Ti 8Al-1V-1Mo at 482°C (900°F) with rotating beam specimens has shown that chromium-molybdenum does not reduce the fatigue strength. Figure 34 presents some of the data accumulated by P&WA on chromium-molybdenum and other coatings. Tiduran™, a nitride type coating, caused substantial reductions in the fatigue strength much of which could be regained by peening or vapor blasting to remove loose corrosion products. Electroless nickel also caused a significant reduction in fatigue strength while both anodizing (as described in Reference 3) and chromium-molybdenum coating did not cause reduction. The major disadvantage with these tests is the relatively small area of the specimen being tested. The hour-glass shape concentrates the stress in one location. To avoid this condition and to allow the testing of relatively large coated areas, a constant stress fatigue specimen was selected for use in this portion of the program.

Specimen Construction

Figure 35 illustrates the general shape and dimensions of the specimen selected. As seen from that figure, the strain remains constant throughout the gage section allowing the testing of coatings over a large area. The strains were measured by strain gages placed as shown.

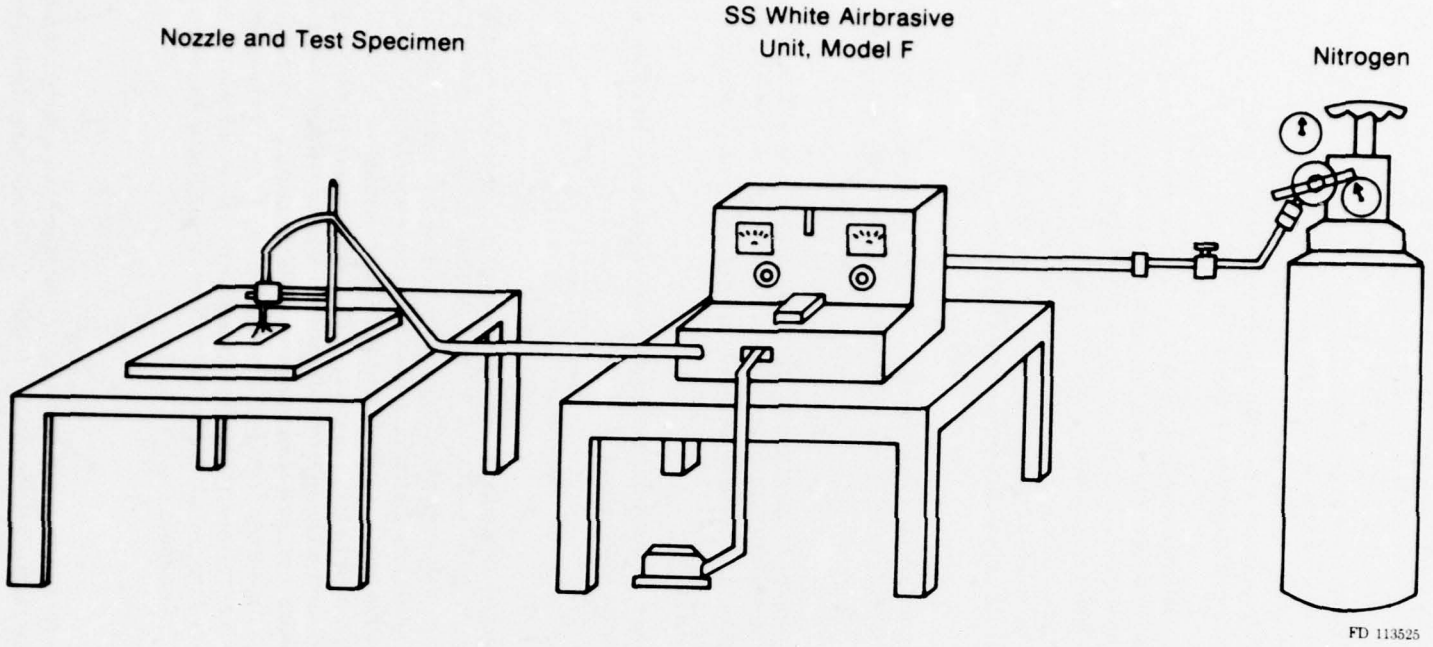

Figure 32. Erosion Test Rig

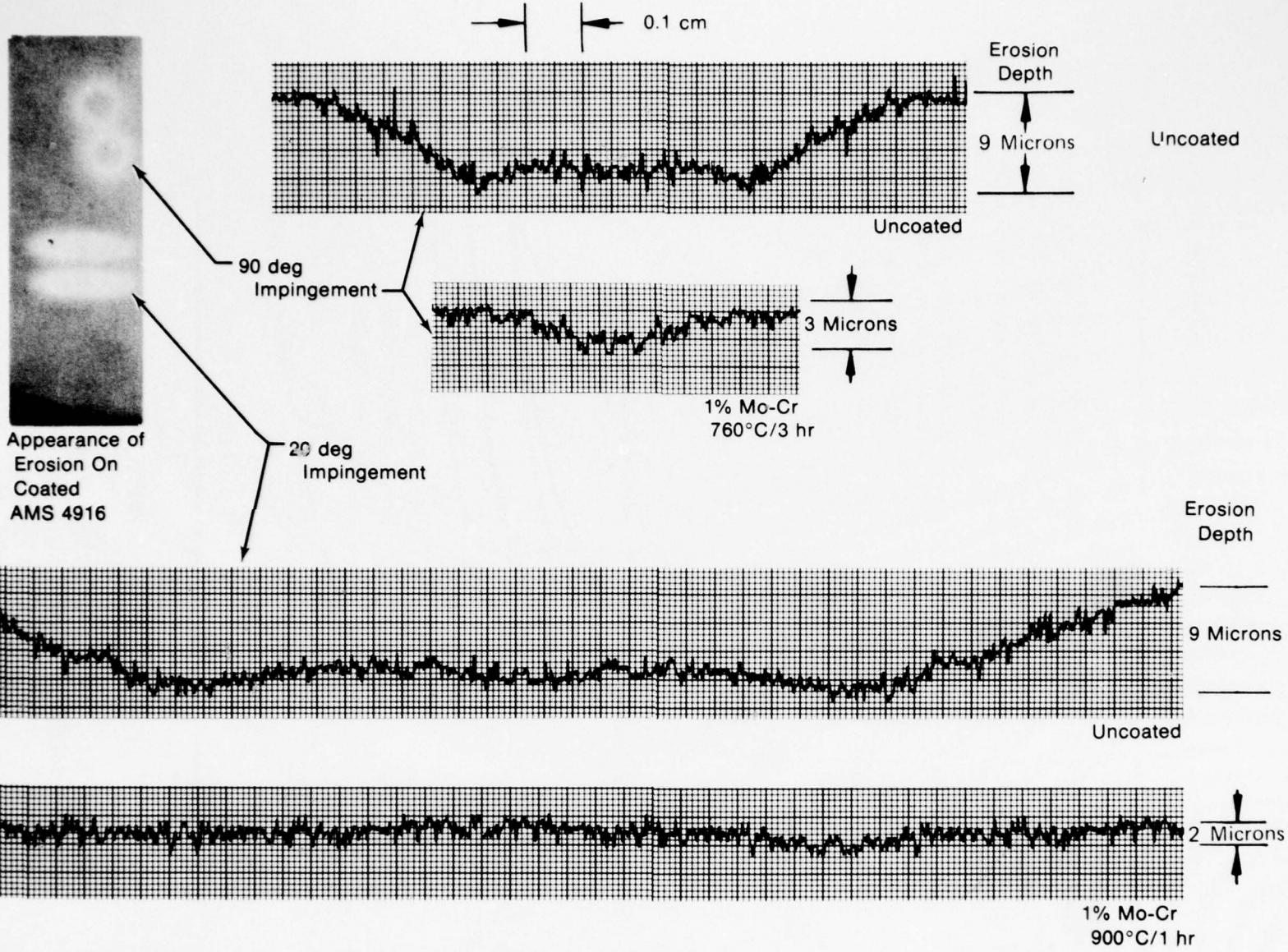

Figure 33. Measurement of Erosion Depth Using Surface Profilometer Traces

FD 113524

TABLE 19. IMPINGEMENT EROSION TESTING OF CHROMIUM-MOLYBDENUM COATED AMS 4916

	Depth of Erosion, microns				
	Impingement Angle				
Specimen Description	*90 deg*		*20 deg*		*Equipment Parameters*
Uncoated	12	11 av.	5	7 avg	Test Rig: SS White Industrial
Ti-8-1-1	9		9		Airbrasive Unit Model F
3% Molybdenum	5	4.5 av.	4	3.5 avg	Nozzle to Specimen Distance: 1.90 cm
760C/3 hr	4		3		(0.75 in.)
1% Molybdenum	3	5 av.	3	3.5 avg	Flowrate: 0.52 g/min.
760C/3 hr	7		4		Nozzle ID: 0.066 cm (0.026 in.)
1% Molybdenum	4	4 av.			Hopper Vibrator Setting: 2 units
900C/1 hr	4				

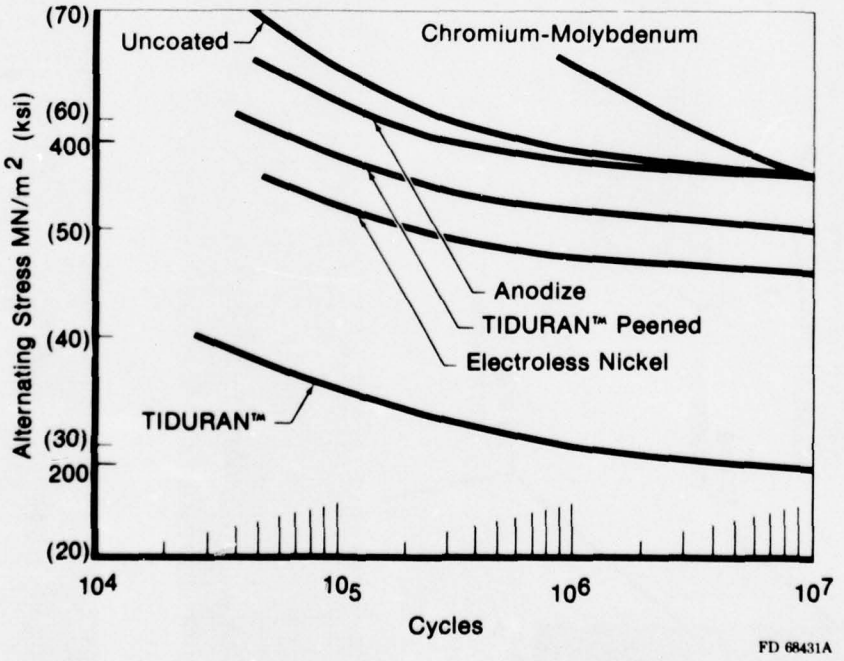

Figure 34. Effects of Coating on High Frequency Fatigue Strength of Ti 8Al-1Mo-1V at 482°C

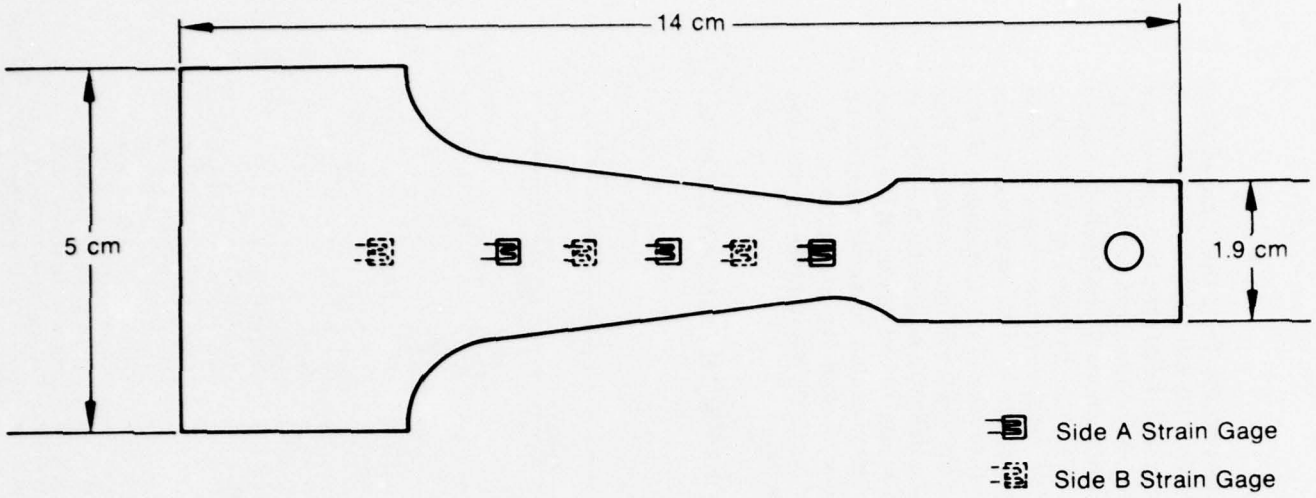

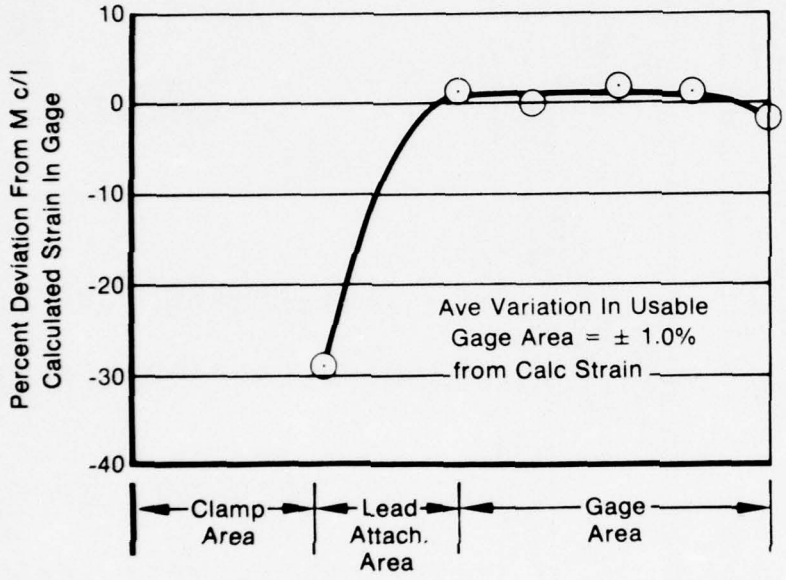

FD 113529

Figure 35. Strain Survey of Constant Stress (Strain Fatigue Specimen)

Chromium-molybdenum coatings were plated only on one side of the fatigue specimen so any improvements in the strength which might be realized from the heat treat would be noted as that, rather than an effect of the coating system. Further, with only one side coated, post-test inspection can identify the side of fatigue failure origin. This information provides added value to studies such as this, investigating the effects of coatings on fatigue strength.

Fatigue Test Results

Table 20 presents a complete summary of the fatigue test results. From the initial series of tests on uncoated specimens at 25°C (77°F) a stress of 379 MN/m² (55 ksi) was selected to test all the coated samples. This stress should always result in a specimen failure but not in so short a time that coating effects cannot be determined. Raising the test temperature to 315°C (600°F) reduced the life of uncoated specimens as expected. Figure 36 illustrates all the results tabulated in Table 20. Generally a slight reduction in fatigue strength could be noted at either room temperature or 315°C (600°F). The 760°C/1% Mo coated specimens ran longer at room temperature than uncoated specimens and a 3% Mo coated specimen with no diffusion cycle lasted longer when tested at 315°C (600°F) than did the other specimens. Comparing all the results of coated specimens with an uncoated S/N curve and the 97.5% minimum regression line commonly used to account for experimental error (Figure 37), indicates no obvious reduction of fatigue strength. However, since most failures on the coated specimens originated on the coated side (Figure 38) it appears coating had some effect, probably related to either microstrain differences in coating/base metal combinations or vacancies created by interdiffusion. Fortunately, this effect is so small that other less sensitive test methods would probably not have detected this difference and it should not be of a major concern.

TABLE 20. HIGH-FREQUENCY FATIGUE RESULTS OF CHROMIUM-MOLYBDENUM COATING

Base Material: AMS 4916
Test Temperatures: 25°C (77°F) and 315°C (600°F)
Cyclic Stress Frequency: 100 Hz

Temperature, °C	(°F)	*Stress,* MN/m²	(ksi)	*Mo Coating,* %	*Diffusion Cycle,* °C/hr	*Cycles*	*Results*
25	(77)	379	(55)	-	-	1×10^7	Did Not Fail
25	(77)	482	(70)	-	-	8.1×10^4	Failed
25	(77)	448	(65)	-	-	1.6×10^5	Failed
25	(77)	413	(60)	-	-	1.38×10^5	Failed
25	(77)	413	(60)	-	-	1.54×10^5	Failed
25	(77)	379	(55)	-	-	3.76×10^5	Failed
25	(77)	344.5	(50)	-	-	1.0×10^7	Did Not Fail
25	(77)	379	(55)	-	-	3.7×10^5	Failed
315	(600)	379	(55)	-	-	1.42×10^5	Failed
315	(600)	344.5	(50)	-	-	1.53×10^5	Failed
315	(600)	344.5	(50)	-	-	2.76×10^5	Failed
315	(600)	344.5	(50)	-	-	1.74×10^5	Failed
25	(77)	379	(55)	1	760/1	1.0×10^7	Did not Fail
25	(77)	379	(55)	1	760/3	1.0×10^7	Did Not Fail
25	(77)	379	(55)	1	815/1	1.92×10^5	Failure Origin: Coated Side
25	(77)	379	(55)	1	815/1	1.98×10^5	Failure Origin: Coated Side
25	(77)	379	(55)	1	871/1	1.9×10^5	Failure Origin: Coated Side
25	(77)	379	(55)	1	871/1	1.51×10^5	Failure Origin: Coated Side
25	(77)	379	(55)	1	927/1	1.32×10^5	Failure Origin: Coated Side
25	(77)	379	(55)	1	927/1	1.63×10^5	Failure Origin: Coated Side
25	(77)	379	(55)	1	871/1 + 593/8	2.36×10^5	Failure Origin: Coated Side
25	(77)	379	(55)	1	871/1 + 593/8	2.08×10^5	Failure Origin: Coated Side
315	(600)	379	(55)	1	760/3	9.49×10^4	Failure Origin: Coated Side
315	(600)	379	(55)	1	760/3	6.49×10^4	Failure Origin: Both Sides
315	(600)	379	(55)	3	-	1.0×10^7	Did Not Fail
315	(600)	379	(55)	3	871/1 + 593/8	1.04×10^5	Failure Origin: Both Sides
315	(600)	379	(55)	3	760/3	9.6×10^4	Failure Origin: Both Sides
315	(600)	379	(55)	1	871/1 + 593/8	7.8×10^4	Failure Origin: Coated Side
315	(600)	379	(55)	1	871/1 + 593/8	6.2×10^4	Failure Origin: Coated Side

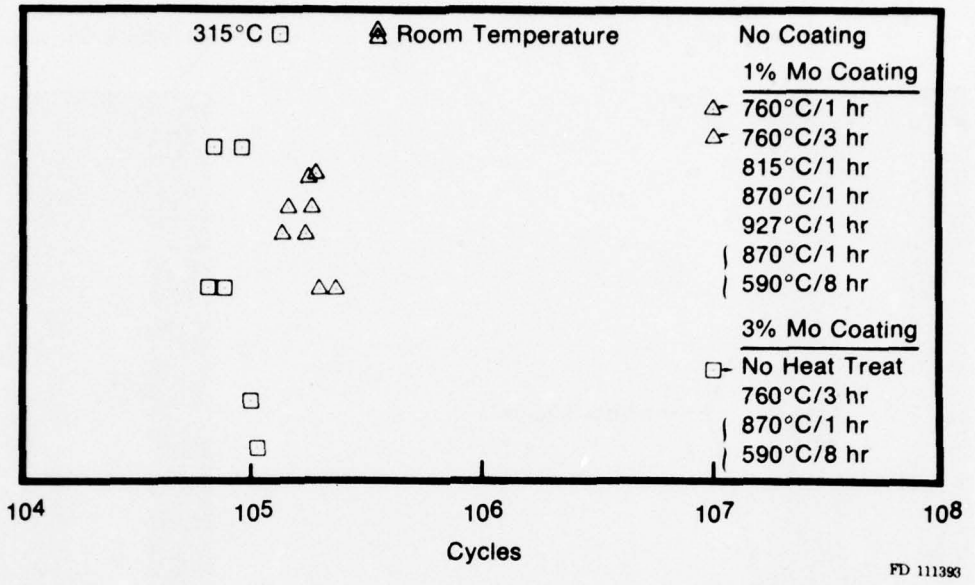

Figure 36. Effects of Coating and Diffusion Cycle on Fatigue Strength of Ti 8Al-1V-1Mo

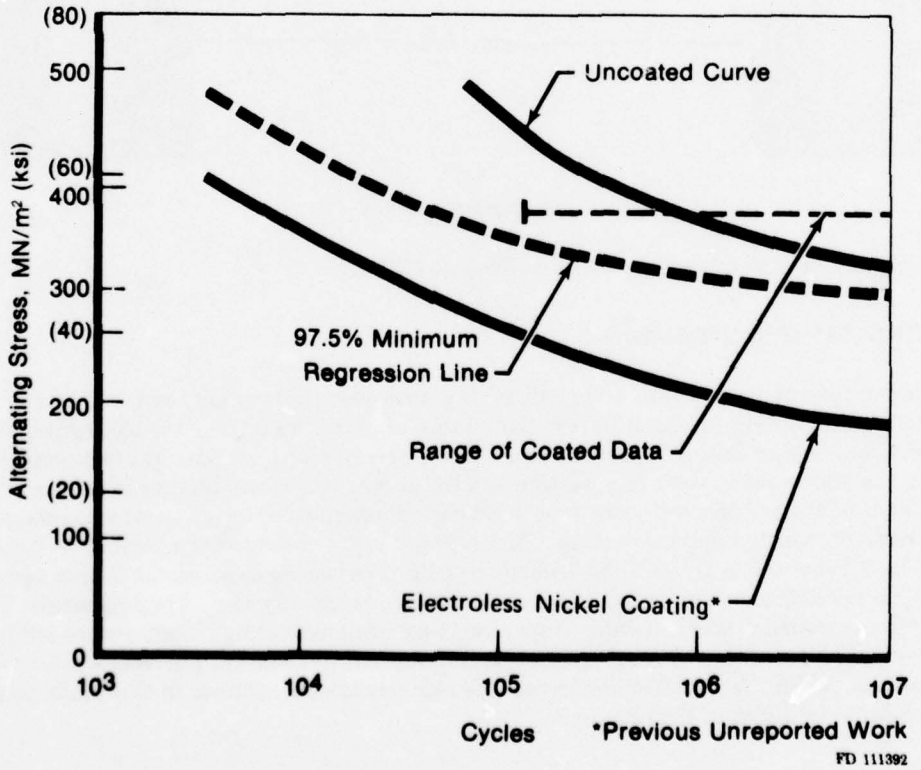

Figure 37. Effect of Chromium-Molybdenum Coating on Fatigue Properties of Ti 8Al-1V-1Mo

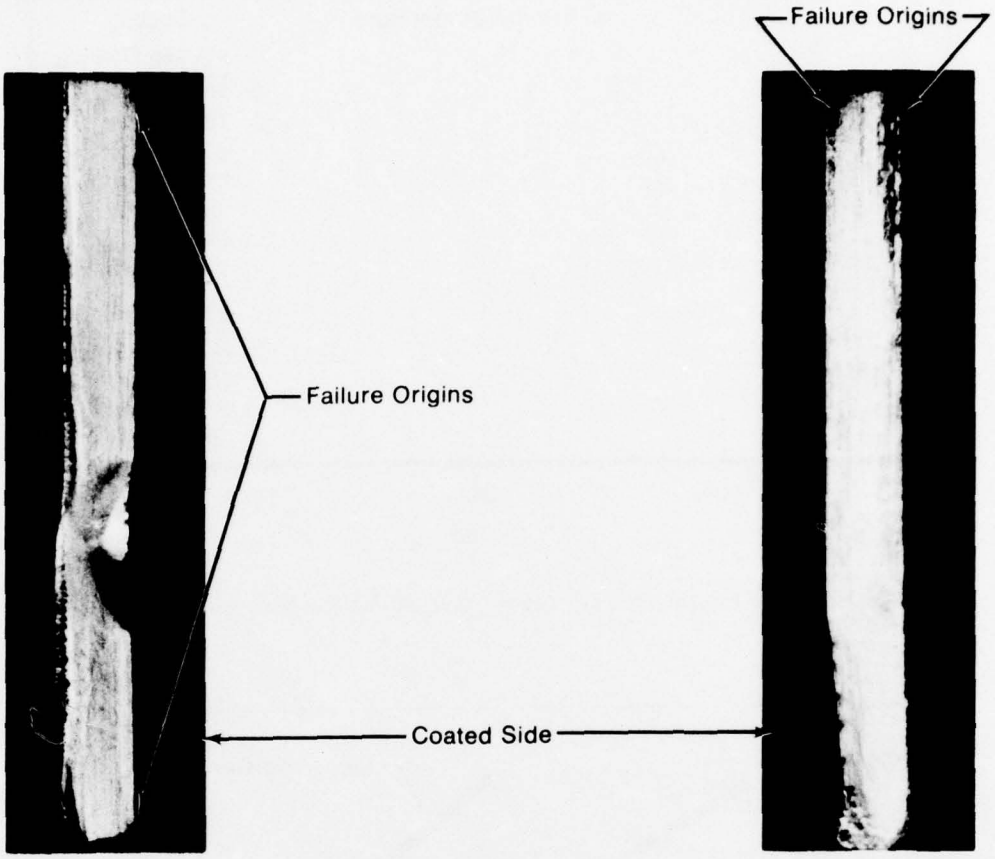

Figure 38. Typical Fracture Faces of Fatigue Failures

FRETTING-FATIGUE STRENGTH

Under conditions of fretting or galling, the optimum coating may not be the one which exhibits the best fatigue strength. Wear characteristics as well as effect on fatigue strength must be considered. Earlier testing conducted on a P&WA developed fretting-fatigue test system which assesses the resistance to wear of a coating system in terms of the reduction in fatigue strength due to a standard set of wear conditions (fretting), showed substantial improvements possible with a chromium-molybdenum coating. The test specimens consisted of a cantilever beam 12.7 by 1.27 by 0.254 cm (5.00 by 0.500 by 0.100 inch) long. The test rig exposed the fatigue specimens to a 50 ksi bearing load applied to the location of maximum vibratory bending stress. The rig permitted controlled elevated temperature operating while providing closely controlled bearing loads over a predetermined specimen area. Figure 39 illustrates some of the results obtained with this previous testing. A modified version of this test was selected for use in this study to permit the evaluation of different bearing loads.

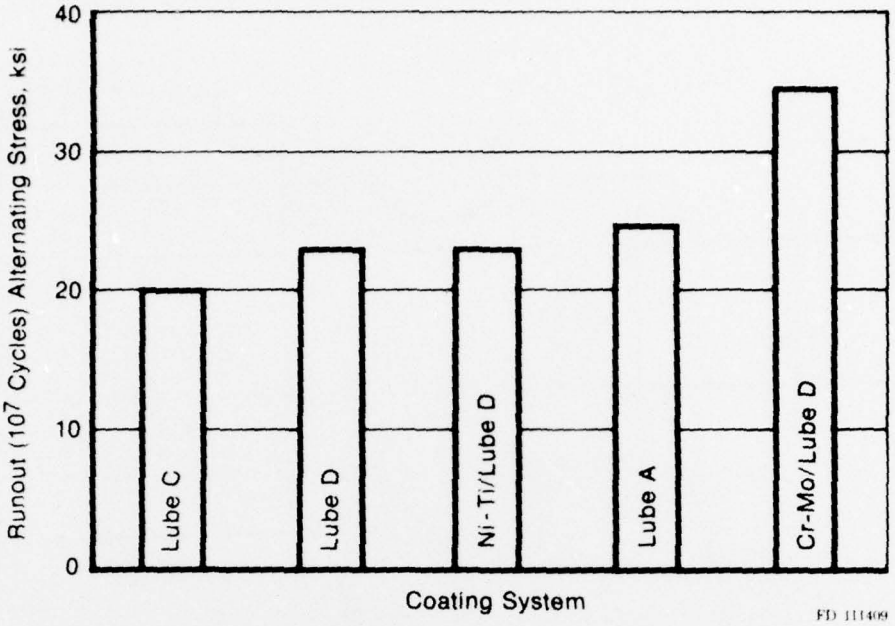

Figure 39. Fretting-Fatigue Testing of Coated Ti 8Al-1V-1Mo at 315°C

Specimen Preparation

The test specimens consisted of a Ti 8Al-1V-1Mo bar 1.27 cm (0.5 in.) by 12.7 cm (5 in.) by 0.254 cm (0.1 in.) thick. Coatings were applied on both sides using the established procedures. Dry film lubricants were used over the chromium-molybdenum coatings since previous testing had shown this to be beneficial. The test unit consisted of the equipment depicted in Figure 40. Fretting occurs under the spring loaded clamps while the specimen is fatigued by bending.

Experimental Results

Table 21 summarizes the results of all the fretting-fatigue tests. Uncoated specimens were run with bearing stresses ranging from 1 to 5 ksi without significantly changing the results. Two compositions of chromium-molybdenum coatings (1% and 3%) likewise had little effect on the results with or without dry film lubricants. Specimen inspection (Figure 41) indicated no significant fretting or metal transfer had occurred in spite of the fact tests conducted on previous programs produced fretting. Apparently, the only difference between these tests was the specimen stiffness; previous specimens were slightly thicker than the ones used in this test. To confirm the results were not dependent on fretting, one specimen was run without any coating and without any applied bearing stress. With an alternating stress of 344.7 MN/m² (50 ksi) the specimen failed after 1.32 by 10^6 cycles. This was within experimental error of results obtained with pin loaded specimen and confirmed no effect was being caused by the applied bearing pins.

Although this test method did not provide additional data on the fretting resistance of the chromium-molybdenum coating system, it did lend further evidence to no fatigue strength losses occurring from the coating process. Previous testing under the higher loading conditions did demonstrate the improved fretting resistance obtained by using chromium-molybdenum coatings on titanium alloys.

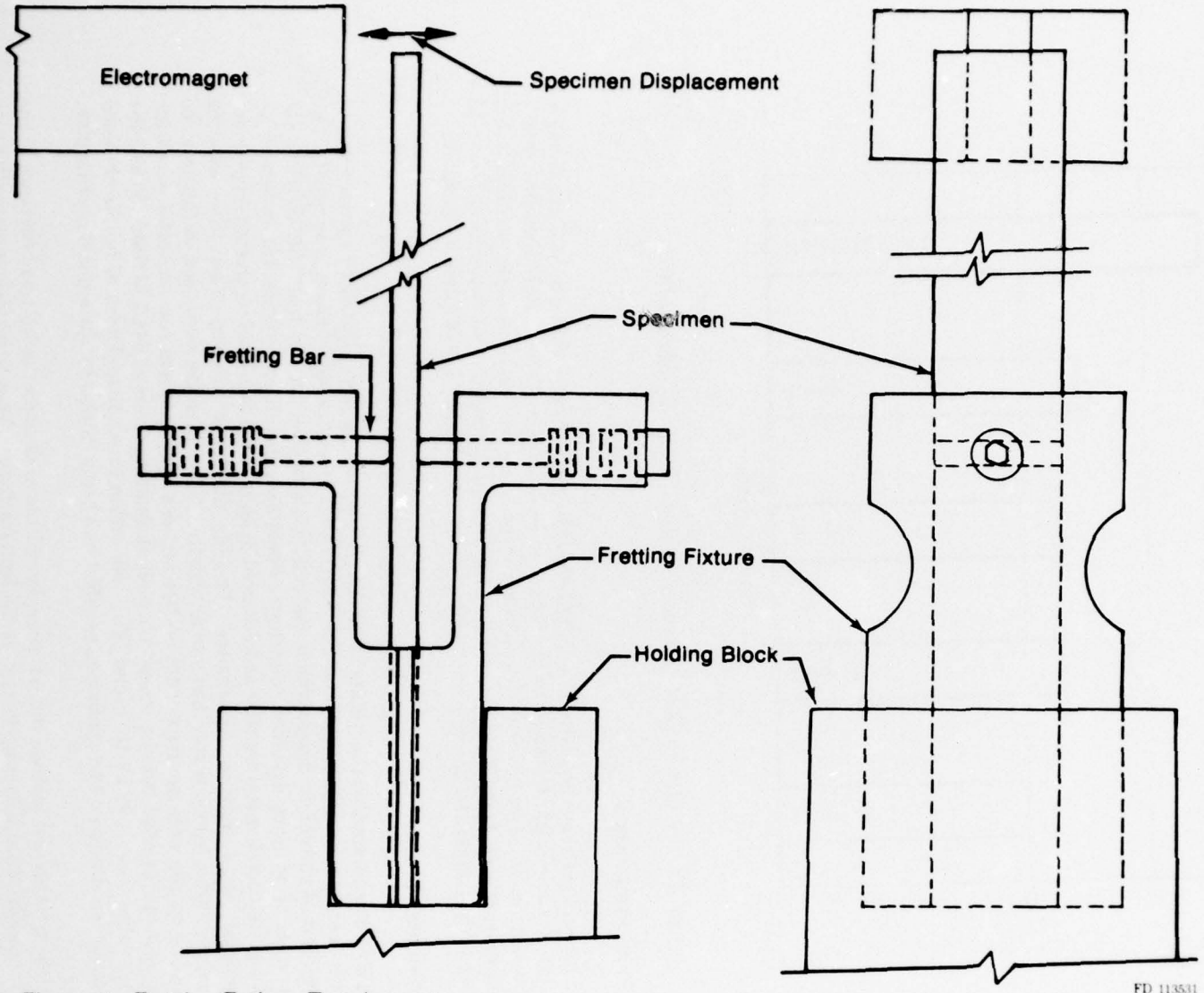

Figure 40. Fretting Fatigue Test Apparatus

TABLE 21. FRETTING FATIGUE TEST RESULTS

All specimens were annealed prior to coating at 593°C (1100°F) for 1 hr

% Mo In Coating	Vapor Blast	Lube B Coated	Diffusion* Treatment	Bearing Stress, MN/m² (ksi)	Alternating Stress, MN/m² (ksi)	Cycles, Hertz	Results
1	X	X	X	17.2 (2.5)	344.7 (50)	6.7×10^4	Failed in gage.
1	X	X	X	17.2 (2.5)	310.3 (45)	1.13×10^5	Failed in gage.
1	X	X	X	17.2 (2.5)	275.8 (40)	2.58×10^6	Failed in gage.
1	X	X	X	17.2 (2.5)	241.3 (35)	1.0×10^7	Did not fail.
3	X	X	X	17.2 (2.5)	310.3 (45)	1.39×10^6	Failed in gage.
3	X	X	X	17.2 (2.5)	275.8 (40)	5.29×10^5	Failed in gage.
3	X	X	X	17.2 (2.5)	344.7 (50)	1.86×10^5	Failed in gage.
3	X	X	X	17.2 (2.5)	241.3 (35)	5.7×10^6	Failed in gage.
				17.2 (2.5)	344.7 (50)	9.8×10^4	Failed in gage.
				6.9 (1.0)	275.8 (40)	3.02×10^6	Failed in gage.
	X	X		17.2 (2.5)	344.7 (50)	9.0×10^5	Failed in gage.
	X	X		17.2 (2.5)	379.2 (55)	2.02×10^5	Failed in gage.
	X	X		17.2 (2.5)	310.3 (45)	7.9×10^5	Failed in gage.
	X	X		17.2 (2.5)	275.8 (40)	7.0×10^6	Failed in gage.
	X			34.5 (5)	344.7 (50)	1.45×10^5	Failed in gage.
	X			34.5 (5)	275.8 (40)	1×10^7	Did not fail.
	X			17.2 (2.5)	275.8 (40)	1×10^7	Did not fail.
	X			17.2 (2.5)	344.7 (50)	1.53×10^5	Failed in gage.
	X			17.2 (2.5)	310.3 (45)	3.4×10^6	Failed in gage.
	X			17.2 (2.5)	310.3 (45)	3.19×10^5	Failed in gage.
	X			17.2 (2.5)	379.2 (55)	7.6×10^4	Failed in gage.
				0	344.7 (50)	1.32×10^5	Failed in gage.

* Diffusion treatment: 871°C (1600°F)/1 hr + 593°C (1100°F)/8 hr.

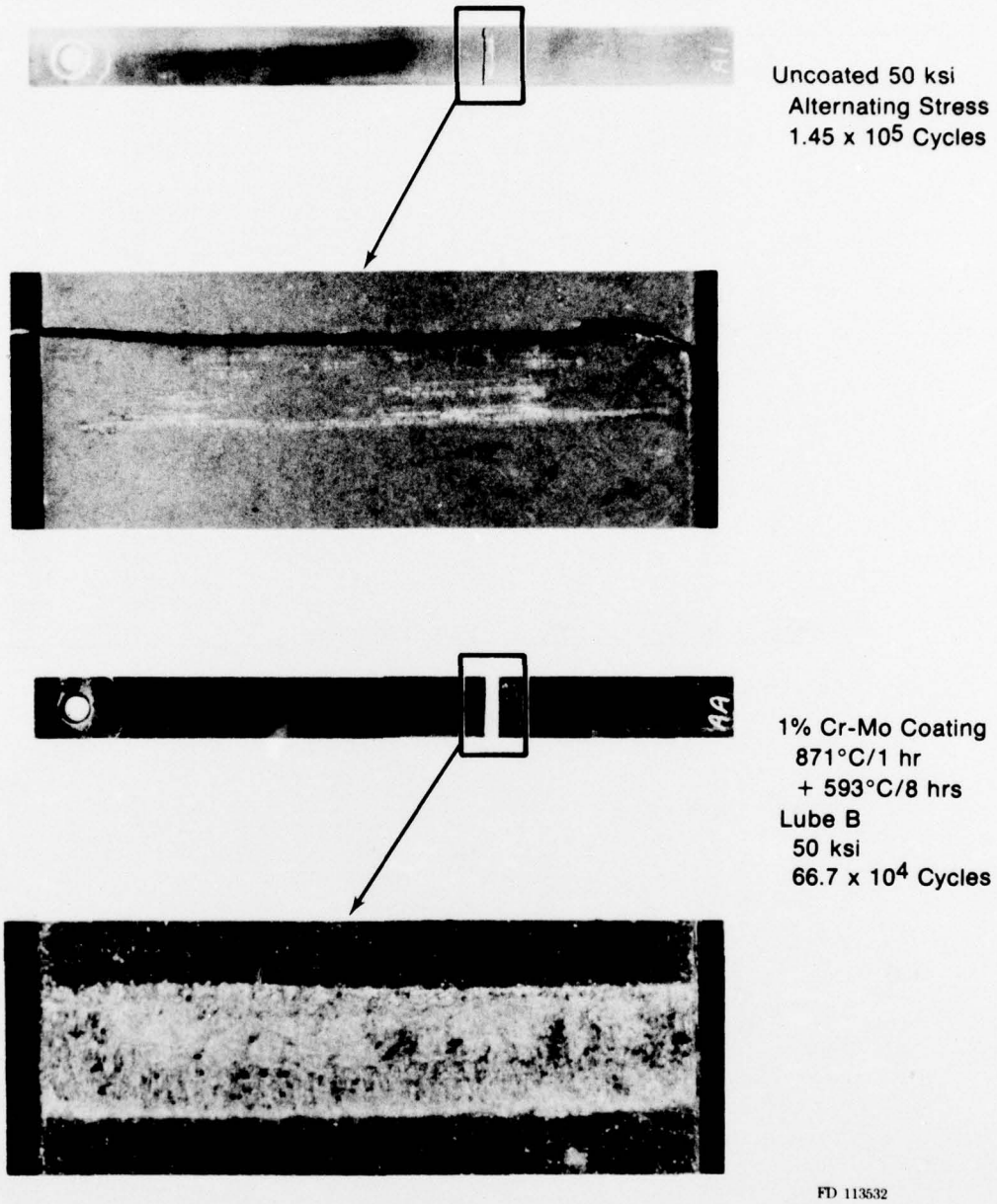

Figure 41. Surface Appearance of Fretting-Fatigue Specimens After Testing at 316°C With a 34.4 MN/m² (5 ksi) Bearing Stress Applied

SECTION III
CONCLUSIONS

COATING APPLICATION

1. A chromium-molybdenum plating solution was developed containing chromic acid, ammonium molybdate, and sulfate ion catalysis. It produced deposits containing 1% molybdenum.

2. Another plating procedure, using periodic on-off current cycling, increased the molybdenum content to 3% and produced fine grain deposits providing improved corrosion resistance.

3. Control of both surface preparation and plating parameters, such as maintaining the solution between 35° and 40°C, were essential to obtain satisfactory deposits.

4. After diffusion at temperatures above 700°C the coatings demonstrated excellent adhesion to the three alloys investigated, Ti 8Al-1V-1Mo, Ti 6Al-4V and Ti 6Al-6V-2Sn.

5. Alternate coating methods such as sputtering can be used to obtain higher concentrations of molybdenum.

COATING PROPERTIES

1. The as-plated coating increases the threshold stress for hot salt stress corrosion cracking at 480°C from below 275 MN/m^2 to above 413 MN/m^2. After diffusion at or above 760°C the coating did not provide the same protection.

2. Either of the deposit compositions, 1% or 3% molybdenum, reduced the room temperature erosion rate to half that of the uncoated alloys.

3. Coatings protected titanium alloy substrates from oxidation at temperatures above 500°C (932°F). The useful operating temperature of coated alloys may be increased by 100°C when only oxidation stability limits the useful application temperatures.

4. Generally, the 1% molybdenum deposit diffused at 760°C for 3 hours provided better wear resistance to titanium alloys than the 3% molybdenum deposits or the higher temperature diffusion cycles. These results indicate the undiffused coating layer provides the bulk of the wear resistance while the diffusion layer is necessary only to improve adhesion.

5. Further lubrication with either oil or dry films improves the wear resistance.

COATING EFFECTS ON ALLOY PROPERTIES

1. None of the chromium-molybdenum alloy coating systems reduced the fatigue strength by more than 3%, regardless of the diffusion cycle used.

2. The coating systems improve the fretting-fatigue strength of titanium alloys.

SECTION IV
RECOMMENDATIONS

The second phase of this study should be started and include:

1. Wear tests, similar to those conducted in this report, on the higher molybdenum containing sputtered coatings.

2. An evaluation of the hot-salt stress corrosion resistance of duplex coated specimens, replated after initial diffusion, to see if both adhesion and stress corrosion resistance can be obtained. Identify the protective mechanism.

3. Complete the evaluation of laser diffusion processes including metallographic examination of processed specimens.

4. Evaluate the extent of distortion caused by the 760°C diffusion process on close tolerance parts.

5. Conduct fatigue and notched fatigue tests at up to 500°C (932°F).

6. Assess the fretting-fatigue resistance of coated titanium using a different test method.

7. Conduct stress rupture, creep, and tensile tests to assess the effects of the coating process on these properties.

8. Evaluate the effects of coating thickness on wear resistance and identify wear mechanisms.

APPENDIX A
CHROMIUM-MOLYBDENUM APPLICATION PROCEDURE

1.0 SOLUTION MAKEUP

1.1 Self-Regulating Plating Bath

Chromic Acid [1]	40 oz/gal (300 g/l)
Ammonium Molybdate $(NH_4)_6 Mo_7O_{24} \times 4 H_2O$	1% Molybdenum deposit-10 oz/gal (75 g/l)
	3% Molybdenum deposit-12.6 oz/gal (95 g/l)

1.1.1 Dissolve the chromic acid in deionized water at room temperature.

1.1.2 Dissolve the ammonium molybdate solution in deionized water at 60°C ± 5°C (140°F ± 10°F).

1.1.3 Add the ammonium molybdate solution to the chromic acid and bring up to the operating level.

1.1.4 Adjust temperature of plating solution to 38°C ± 2°C (100°F ± 5°F)

1.2 Vapor Blast

Novaculite 200 [2]	480-720g/l (4 to 6 lb/gal)
Antisolidifying Compound [3]	113g/22.7Kg (4 oz/50lb) abrasive
Corrosion Inhibitor [4]	4 ml/l (15 ml/gal)

1.2.1 Fill tank to about ¾ of operating level with water.

1.2.2 Add abrasive slowly while circulating pump is on.

1.2.3 Add antisolidifying compound.

1.2.4 Add corrosion inhibitor.

1.2.5 Fill to operating level.

1.3 Etch Solution

Hydrofluoric Acid (48%)	2.1 ml/l (8 ml/gal)
Sodium Chromate	11.7 ml/l (1.5 oz/gal)

1.3.1 Dissolve the required amount of sodium chromate in deionized water.

1.3.2 Add required amount of hydrofluoric acid.

2.0 PROCEDURE

2.1 Mask area not to be plated with suitable stop-off lacquer

2.2 Vapor blast surface to be plated with wet abrasive at 0.4 to 0.7 MPa (50 to 100 psi)

2.3 Rinse thoroughly in clean running water.

2.3.1 Cleaned surface must not be allowed to dry prior to plating. Submerge part in deionized water.

2.4 Etch for 5 to 10 seconds to produce chrome conversion coating

2.5 Using lead anodes, immerse part in plating solution with current "off"

2.6 Raise current to 11.7 ASD (0.75 ASI) for 2.5 minutes

2.7 Plate at 46.7 ASD (3.0 ASI) for 30 minutes

2.7.1 To deposit a 3% molybdenum concentration, periodically interrupt current 1 second on, 1 second off at 46.7 ASD (3.0 ASI) for 30 minutes. (Note: use 94.5 g/l (12.6 oz/gal) of ammonium molybdate make-up solution in conjunction with periodic interrupt method.)

2.8 Rinse thoroughly in deionized water

2.9 Heat treat in vacuum at 760°C for 3 hours

3.0 (Option) glass bead peen or vapor blast surfaces.

NOTE:

[1] United Chromium, SRHS CR 110
[2] Vapor Blasting Mfg. Co., NVB #200
[3] Vapor Blast Mfg. Co., No-Pak
[4] Reilly-Whiteman-Walton Co., X61-60 water conditioner

APPENDIX B
METHOD FOR DETERMINING THE EFFECTS OF HOT-SALT STRESS CORROSION ON TITANIUM ALLOYS

1. SCOPE

This section describes the procedure for determining the effect of materials and processes on stress corrosion of titanium test pieces.

2. APPARATUS

2.1 Stress Corrosion Test Specimens: Ti 8Al-1V-1Mo sheet, variable length 0.10 ± 0.02 cm thick, 1.25 cm wide.

2.1.1 Stress will be calculated for the specimens using methods described in Reference 20.

2.2 Specimen Holder: Figure 42.

2.3 Oven: Circulating air, capable of heating to and maintaining 480°C ± 5°C (900° ± 10°F) for 100 hr.

2.4 Microscope: Capable of 10X magnification.

2.5 Microsyringe: Capable of measuring 150 ± 5 microliters.

2.6 Sodium Chloride Solution: 3% aqueous solution of sodium chloride prepared with distilled or demineralized water.

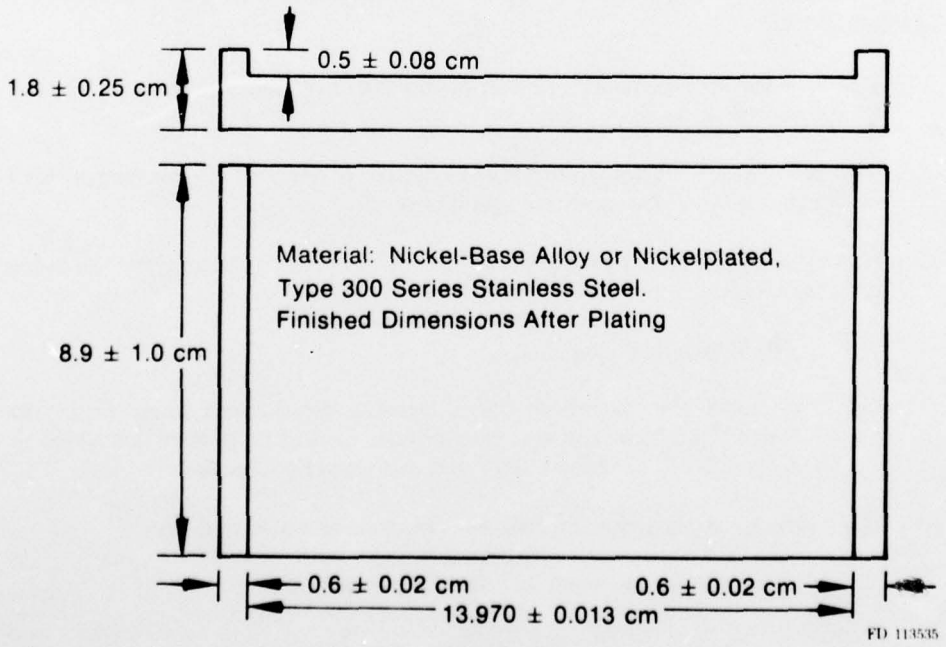

Figure 42. Stress Corrosion Specimen Holder

3. PROCEDURE

3.1 For Chromium-Molybdenum Coated Specimens

3.1.1 Clean the test specimens and a control specimen (not treated) with acetone. Use white gloves or the equivalent when handling specimens to prevent contamination.

3.1.2 Bend the test specimens and one control specimen into the specimen holder.

3.1.3 Place 150 ± 5 microliters of 3% sodium chloride solution from a microsyringe onto an approximately 1-inch long section of each specimen. The solution should be placed near the center and on the convex side of the specimens.

3.1.4 Dry at 80 to 90°C. A solid residue shall remain on the specimens.

3.1.5 Place the holder with the Ti 8Al-1V-1Mo specimens into a clean circulating air oven at the desired temperature for 100 hr.

3.2 For All Other Surface Treatments

3.2.1 Clean a control specimen (not treated) with acetone. Use white gloves or the equivalent when handling specimens to prevent contamination.

3.2.2 Bend the test specimens treated with the material or process being tested and one control specimen into the specimen holder.

3.2.3 Place the holder with the Ti 8Al-1V-1Mo specimens into a clean circulating air oven at the desired temperature for 100 hr.

4. EXAMINATION

4.1 Examine the specimens at 7 to 10X for breaks or obvious cracks while they are still in the specimen holder.

4.2 Test is invalid if control specimen does not break or show obvious cracks. Repeat all tests using new control and test specimens.

4.3 If control or test specimen shows no breaks or cracks, remove from the holder and treat as follows.

4.3.1 Vapor blast the specimen.

4.3.2 Immerse the specimen into a solution of: 5 parts nitric acid, one part hydrofluoric acid and one part sulfuric acid at 50 to 65°C for 30 sec or until excessive red fumes are liberated, whichever comes first.

4.3.3 Immediately rinse the specimen in running water and dry.

4.3.4 Examine the specimen at 7 to 10X for cracks.

5. RECORDING AND REPORTING

5.1 Test Specimen Showing Breaks or Cracks: Record and report, "Test specimens show evidence of breaks or cracks. Test specimens fail to pass the stress corrosion test."

5.2 Test Specimen Showing No Evidence of Cracks: Record and report, "Test specimens pass the stress corrosion test."

5.3 Control Specimen Shows No Evidence of Cracks: Record, "Test not valid. Control specimens show no evidence of cracks."

REFERENCES

1. Krienke, R. D., "Plating Wear-Resistant Coatings on Titanium," *Metal Progress*, June 1969

2. Jacquet, P. A. et al, "Influence of Surface Conditions on the Rubbing Abrasion of Electrolytic Deposits of Hard Chromium and Chromium-Molybdenum Alloys," *Revue de Metallurgie* Vol. 56, p. 135, 1959

3. Manty, B. A., J. P. Winfree, S. Bonifazi, *Corrosion Resistant Anodic Coatings for Titanium* AFML-TR-75-42, Vol. 1, p. 463, September 1975

4. Nejedlik, J. F., *Protective Coatings for Titanium Alloy Compressor Blades*, TRW Report-4580, December 1970

5. Gulbransen, E. A. and K. F. Andrew, "Kinetics of the Reactions of Titanium with O_2, N_2 and H_2," *Transactions of American Institute of Mechanical Engineers*, October 1949

6. McComas, C. C. and L. S. Sokol, *Research for Engine Demonstration of Erosion-Resistant Coating Effectiveness*, Army Material and Mechanics Research Center CTR 74-9, March 1974

7. Manty, B. A., *Compressor Coatings Development and Evaluation*, Pratt & Whitney Aircraft Group, Government Products Division Report FMDL 15587, January 1972

8. Schwartz, R., *Development of Improved Corrosion Protection for Long Time Exposure of S-11 Stage and/or Hardware*, Final Report NAS-7-200, December 1971

9. Stein, B. A. and H. G. Dexter, *Coatings and Surface Treatments for Longtime Protection of Ti 8Al-1V-1Mo Alloy Sheet from Hot-Salt-Stress-Corrosion*, NASA TND-4319, March 1968

10. Groves, M. T., *Environmental Protection to 922°K (1200°F) for Titanium Alloys*, NASA CR-134537, November 1973

11. Brenner and Ogburn, *Journal of the Electrochemical Society*, Vol. 96, p. 347, 1949

12. Muller, E., *Zeitschrift für Elektrochemie*, Vol. 50, p. 172, 1944

13. Briggs, J. Z. and H. W. Scherltz, *Plating*, Vol. 46, p. 1370, 1959

14. Ma, C. C., U. S. Patent 2,516,227 (July 1950)

15. Shenoi B. A. and K. S. Indira, "Electrodepositing of Chromium Molybdenum Alloys," *Metal Finishing*, p. 56, May 1965

16. Wilms, G. R., "Preliminary Investigations on the Properties of Chromium and Chromium Alloys at Elevated Temperatures," *Journal of the Institute of Metals*, Vol. 87, pp. 77-78, 1958-1959

17. Holt, M. L. and D. W. Ernst, Progress Report No. 1, May 8, 1952 to Office of Ordnance Research Contract DA11-022-ORD-656

18. Jacquet, P. A. et al, "The Influence of the Surface Structure on the Attrition of Hard Chromium and Mixed Chromium-Molybdenum Deposit," *Chrome GMELINS Handbook of Inorganic Chemistry*, pp. 46-58 (1959-1960)

19. Krishnan, R. M., "Electrodeposition of Chromium-Self Regulating Tetrachromate Baths," *Metal Finishing*, April 1975

20. Haaijer & Loginow, "Stress Analysis of Bent Beam Stress Corrosion Specimen," *Corrosion* Vol. 21, No. 4, p. 105 (1965)

21. *Progress Report on the Salt Corrosion of Titanium Alloys at Elevated Temperature and Stress*, TML Report No. 88, Battelle Memorial Institute, 1957

22. *The Science, Technology, and Application of Titanium*, Pergamon Press, 1970

23. Anon, *Corrosion*, L. L. Shreir, J. Wiley & Sons, 1963

24. Boyd, W. K., *Stress Corrosion Cracking of Titanium and Its Alloys*, DMIC Memorandum No. 234, Battelle Memorial Institute, 1968

25. Gray, H. R., *Hot-Salt Stress Corrosion of Titanium Alloys: Generation of Hydrogen and Its Embrittling*, NASA TN D-5000, 1969

26. Dix, E. H., Transactions American Institute Mining (Metallurgical) Engineers, Vol. 11, p. 137, 1940

27. Keating, F. H., "Internal Stresses in Metals and Alloys," *Institute of Metals*, London, p. 311, 1948

28. Evans, U. R., *Corrosion*, Vol. 1, p. 238, 1951

29. Logan, H. L., Journal of Research of the National Bureau of Standards, Vol. 48, p. 99, 1952

30. Hoar, T. P. and J. G. Hines, Standards Institution of Israel, Vol. 182, p. 124, 1956

31. Beck, T. R., "Electrochemical Mechanism in the Stress Corrosion Cracking of Titanium Alloys," *The Science, Technology and Application of Titanium*, Pergamon Press, 1970

32. Ondrejcin, R. S., "Hydrogen in Hot-Salt Stress Corrosion Cracking of Titanium Aluminum Alloys," *Transactions American Institute of Mining, Metallurgical and Petroleum Engineers*, Vol. 1, p. 3031, 1970

33. Evans, U. R., *Stress Corrosion Cracking and Embrittlement*, Wiley, New York 1956

34. Powell, D. T. and J. C. Scully, "The Stress Corrosion Cracking of Alpha Titanium Alloys at Room Temperature," *The Science, Technology and Application of Titanium*, Pergamon Press, 1970

35. Ridout, S. P., R. S. Ondycin and M. R. Louthan, Jr., "Hot-Salt Stress Corrosion Cracking of Titanium Alloys," *The Science, Technology and Application of Titanium*, Pergamon Press, 1970

36. Hines, J. G., "Theories of Stress Corrosion," *Corrosion*, L. L. Shreir, Wiley 1963

37. Kofsted, P., K. Hauffe, and H. Kjollendal, *Acta Chemica Scandinavica*, Vol. 12, p. 239, 1958

38. Kofsted, P., *High Temperature Oxidation of Metals*, John Wiley & Sons, pp. 166-178, 1966

39. Ferguson, J. M., *Oxidation and Contamination of Titanium and its Alloys*, DMIC Memorandum No. 238, Battelle Memorial Institute, July 1968

40. Shamblen, C. E. and T. K. Redden, "Air Contamination and Embrittlement of Titanium Alloys," *The Science, Technology and Application of Titanium*, Pergamon Press, p. 199, 1970

41. Breman, E. M. et al, "Processing Materials with Lasers," *Physics Today*, p. 44, November 1976

42. Mouchan, B. A. and A. V. Demchishin, *Fiz. Metal. Metalloved*, 28, No. 4, 653-660, 1969

43. Manty, B. A., Aircraft Engine Cleaning, Presented at Corrosion/77, March 14-18, 1977 (Preprint No. 75).